Evolution of Mating Systems in Basidiomycetes and the Genetic Architecture Underlying Mating-Type Determination in the Yeast *Leucosporidium scottii*

Teresa M. Maia,* Susana T. Lopes,* João M. G. C. F. Almeida,* Luiz H. Rosa,† José Paulo Sampaio,* Paula Gonçalves,* and Marco A. Coelho*,[1]

*UCIBIO, REQUIMTE, Departamento de Ciências da Vida, Faculdade de Ciências e Tecnologia, Universidade Nova de Lisboa, 2829-516 Caparica, Portugal, and †Departamento de Microbiologia, Universidade Federal de Minas Gerais, Belo Horizonte, MG, 31270-901 Brazil

ORCID ID: 0000-0002-5716-0561 (M.A.C.)

ABSTRACT In most fungi, sexual reproduction is bipolar; that is, two alternate sets of genes at a single mating-type (*MAT*) locus determine two mating types. However, in the Basidiomycota, a unique (tetrapolar) reproductive system emerged in which sexual identity is governed by two unlinked *MAT* loci, each of which controls independent mechanisms of self/nonself recognition. Tetrapolar-to-bipolar transitions have occurred on multiple occasions in the Basidiomycota, resulting, for example, from linkage of the two *MAT* loci into a single inheritable unit. Nevertheless, owing to the scarcity of molecular data regarding tetrapolar systems in the earliest-branching lineage of the Basidiomycota (subphylum Pucciniomycotina), it is presently unclear if the last common ancestor was tetrapolar or bipolar. Here, we address this question, by investigating the mating system of the Pucciniomycotina yeast *Leucosporidium scottii*. Using whole-genome sequencing and chromoblot analysis, we discovered that sexual reproduction is governed by two physically unlinked gene clusters: a multiallelic homeodomain (*HD*) locus and a pheromone/receptor (*P/R*) locus that is biallelic, thereby dismissing the existence of a third *P/R* allele as proposed earlier. Allele distribution of both *MAT* genes in natural populations showed that the two loci were in strong linkage disequilibrium, but independent assortment of *MAT* alleles was observed in the meiotic progeny of a test cross. The sexual cycle produces fertile progeny with similar proportions of the four mating types, but approximately 2/3 of the progeny was found to be nonhaploid. Our study adds to others in reinforcing tetrapolarity as the ancestral state of all basidiomycetes.

KEYWORDS sexual reproduction; mating type; mating-type determination; fungi; Basidiomycota

SEXUAL reproduction has a pivotal role in the biology of many eukaryotes and is likely a defining evolutionary innovation of this lineage (Dacks and Roger 1999; Goodenough and Heitman 2014). In addition to promoting genetic variation, required for adaptation to fluctuating environments and long-term survival, sexual reproduction in many fungal species, in particular, has a central role in pathogenic development (Bakkeren *et al.* 2008; Nadal *et al.* 2008; Heitman 2010; Heitman *et al.* 2014). It is thus not surprising that recent advances in genome sequencing have revealed that most fungal species have retained the machinery for sexual reproduction and meiosis (Halary *et al.* 2011; Dyer and O'Gorman 2012; Gioti *et al.* 2013; Heitman *et al.* 2014). However, this resilience to keep sexual competence intact comes with an extremely dynamic evolution of sexual behaviors and mating type-determining mechanisms, which may influence important evolutionary and ecological processes, such as adaptation and speciation (Billiard *et al.* 2011; Heitman *et al.* 2013; Nieuwenhuis *et al.* 2013).

In the phylum Basidiomycota, sexual reproduction is often dictated by two independent sets of mating-type (*MAT*)-specific genes that control different stages of the sexual cycle. These genes encode premating lipopeptide pheromones and their cognate receptors (P/R), which mediate recognition of mating partners and cell fusion, and homeodomain transcription

doi: 10.1534/genetics.115.177717
Manuscript received April 29, 2015; accepted for publication July 13, 2015; published Early Online July 14, 2015.
Supporting information is available online at www.genetics.org/lookup/suppl/doi:10.1534/genetics.115.177717/-/DC1.
[1]Corresponding author: UCIBIO, REQUIMTE, Departamento de Ciências da Vida, Faculdade de Ciências e Tecnologia, Universidade Nova de Lisboa, 2829-516 Caparica, Portugal. E-mail: madc@fct.unl.pt

factors (HD1 and HD2) that form heterodimers that regulate postmating behavior (Kües *et al.* 2011; Nieuwenhuis *et al.* 2013). Over the years, it has been shown that basidiomycetes may occur in two different mating configurations: bipolar and tetrapolar. In bipolar species, *P/R* and *HD* genes are genetically linked at a single *MAT* locus and therefore only two mating types are generated after meiosis (referred to as "A1" and "A2" or "**a**" and "α"). In contrast, in tetrapolar species, *P/R* and *HD* genes are located at two physically unlinked genomic regions that segregate independently during meiosis to generate up to four different mating types (Kües *et al.* 2011; Heitman *et al.* 2013; Nieuwenhuis *et al.* 2013). Despite these fundamental differences, individuals that are brought together must carry different alleles at both *MAT* loci for sexual reproduction to occur (reviewed in Kües *et al.* 2011; Nieuwenhuis *et al.* 2013). This condition renders the tetrapolar system less favorable for inbreeding, as the odds to find a compatible mating partner among siblings are reduced to 25% compared to 50% in a bipolar system. Interestingly, most of the known tetrapolar yeast species exhibit a biallelic *P/R* locus and a multiallelic *HD* locus (*viz. Ustilago maydis*, *Kwoniella heveanensis*, *Kwoniella mangrovensis*, *Cryptococcus amylolentus*) (Bölker *et al.* 1992; Kämper *et al.* 1995; Metin *et al.* 2010; Findley *et al.* 2012; Guerreiro *et al.* 2013), a configuration originally designated as "modified tetrapolar" by Robert J. Bandoni to denote that outcrossing in such a system cannot exceed 50% (Bandoni 1963; Kües *et al.* 2011). Indeed, only by evolving multiple alleles at both *MAT* loci can a tetrapolar system maximize the outcrossing efficiency to >50%, as observed in mushroom-forming species (*viz. Coprinopsis cinerea* and *Schizophyllum commune*) (Casselton and Kües 2007).

A large number of basidiomycetes have had their mating system identified, revealing that both tetrapolar and bipolar species are interspersed along the phylum (Heitman *et al.* 2013; Nieuwenhuis *et al.* 2013). However, much of what is known about bipolarity in these species emphasizes that these bipolar states have most likely arisen from a tetrapolar configuration. This can be attained either by (i) loss of function of the *P/R* locus as an incompatibility factor (as, *e.g.*, in *Coprinus disseminatus*, *Pholiota microspore*, and *Phanerochaete chrysosporium*) (Raper 1966; James *et al.* 2006, 2011; Yi *et al.* 2009) or (ii) coalescence of unlinked *P/R* and *HD* loci into a contiguous inheritable unit, with both *MAT* genes remaining functional in mating-type determination. This last scenario was shown to be at the basis of extant bipolar species belonging to two of the three major Basidiomycota lineages, namely *Cryptococcus neoformans* (subphylum Agaricomycotina) (Fraser *et al.* 2004; Findley *et al.* 2012) and *Ustilago hordei* (subphylum Ustilaginomycotina) (Bakkeren *et al.* 2006). In these cases, the *MAT* locus has expanded into a large, nonrecombining region of a chromosome that is usually highly rearranged between the two mating types and rich in repetitive elements (Fraser *et al.* 2004; Bakkeren *et al.* 2006).

The third and earliest-branching lineage of basidiomycetes (subphylum Pucciniomycotina) comprises species with diverse cellular forms and lifestyles (Aime *et al.* 2006). Pioneering studies addressing the molecular basis of mating behavior in this lineage were conducted in *Microbotryum lychnidis-dioicae* (order Microbotryales), an anther-smut fungus in which heteromorphic mating-type chromosomes were first described (Hood 2002; Hood *et al.* 2013). Allocation of the *MAT* pheromone receptor genes to these chromosomes, each carrying the allelic version that confers *MAT* A1 or *MAT* A2 identity (Giraud *et al.* 2008; Petit *et al.* 2012), and the very recent finding of the *HD1/HD2* gene pair at a distance of ∼0.60 Mb apart from the *P/R* genes (Badouin *et al.* 2015), provides conclusive evidence that a bipolar mating system governs sexual reproduction in this species. Additional insight into the evolution of mating systems in the Pucciniomycotina emerged from our studies in a group of red-pigmented saprobic yeast species of the order Sporidiobolales (*viz. Sporidiobolus salmonicolor*) (Coelho *et al.* 2010, 2011). This work uncovered a mating system that appeared to deviate from the classical bipolar and tetrapolar mating paradigms based on two main observations: first, a worldwide collection of natural isolates of *S. salmonicolor* revealed that only two alleles (A1 and A2) exist at the *P/R* locus, each of which appears to be linked to multiple (yet specific) alleles at the *HD* locus; and second, the progeny of a cross between compatible strains indicate that recombination/assortment of *P/R* and *HD* loci may occur, albeit at a low frequency (Coelho *et al.* 2010). Therefore, to denote the distinction between the strictly bipolar mating behavior of *S. salmonicolor* strains isolated from nature and the apparent tetrapolar pattern of inheritance of mating-type genes in laboratory crosses, this mating system was named "pseudo-bipolar" (Coelho *et al.* 2010).

Even though the tetrapolar system appears to be exclusive of the phylum Basidiomycota (Kües *et al.* 2011; Heitman *et al.* 2013; Nieuwenhuis *et al.* 2013), it is currently equivocal if the last common ancestor of the basidiomycetes had a tetrapolar or bipolar mating system. Reconstructing the evolutionary path leading to the present mating systems of basidiomycetes requires obtaining information on this trait for several extant bipolar and tetrapolar members of the three major lineages. This approach, however, has been hindered owing to the scarcity of data for this trait in putative tetrapolar species of the Pucciniomycotina.

Leucosporidium scottii is a Pucciniomycotina yeast species with a typical dimorphic life cycle, comprising heterothallic, homothallic (self-fertile), and apparently asexual individuals (Fell and Statzell-Tallman 1982; Sampaio *et al.* 2003; de Garcia *et al.* 2015). This species belongs to the order Leucosporidiales, which is phylogenetically related to both Sporidiobolales (red yeasts) and Microbotryales (anther-smuts) (Sampaio *et al.* 2003; Aime *et al.* 2006). Early studies by Fell and co-workers aimed at characterizing the mating system of this species had already suggested the presence of a multiallelic tetrapolar system, with at least five and three mating specificities, respectively, for the inferred *MAT* A and *MAT* B loci (Fell and Statzell-Tallman 1982). Remarkably, the authors also reported the apparent generation of new mating factors among the progenies of

laboratory crosses. As previously documented in tetrapolar mushroom species (Raper 1966; Casselton and Kües 2007), this finding was considered as an indication that each factor consisted of more than one locus and that "intrafactor" recombination would generate new *MAT* specificities (Fell and Statzell-Tallman 1982). The *L. scottii* study was the first report of a multiallelic tetrapolar system in the Pucciniomycotina, although subsequent tetrapolar states were described for other species of this lineage, including the obligate plant parasitic rust fungi (Lawrence 1980; Yamazaki and Katsuya 1988; Narisawa *et al.* 1994). Nevertheless, in none of these cases has the molecular basis of the apparent tetrapolar mating behavior been elucidated.

In this study, we provide a detailed molecular characterization of the mating system of *L. scottii*. Using newly generated genome sequence data of two compatible strains, we determined the chromosomal regions harboring *P/R* and *HD* loci and compared them to the corresponding regions of other Pucciniomycotina species. We also confirmed that *P/R* and *HD* loci consist of two physically unlinked gene clusters that localize to different chromosomes. However, this configuration does not seem to translate into a random association of *P/R* and *HD* alleles in natural populations. Finally, our genetic analysis of *L. scottii* meiotic progeny reveals that segregation of *MAT* alleles is not biased toward a particular *MAT* genotype, but a high frequency of apparently nonhaploid progeny is generated. We discuss our findings in the context of the evolution of the tetrapolar mating system in basidiomycetes.

Materials and Methods

Genomic DNA isolation, library preparation, and sequencing

High-molecular-weight genomic DNA was isolated from yeast cells grown on solid MYP medium [0.7% (w/v) malt extract, 0.05% (w/v) yeast extract, 0.25% (w/v) soytone–peptone, 1.5% (w/v) agar] at 17° for 3 days using a modified phenol: chloroform:isoamyl alcohol method (Gonçalves *et al.* 2011). DNA was dissolved in TE buffer (10 mM Tris-HCl, 1 mM EDTA, pH 7.6) with RNase A (100 μg/ml). The genome sequences of two strains of *L. scottii* were generated. For Illumina sequencing, 1 μg of genomic DNA was used to generate paired-end libraries using a manufacturer's kit (TruSeq DNA Prep Kit v2). Additionally, using 10 μg of genomic DNA, Illumina mate-pair libraries were generated and sequenced using the services of a commercial provider (University of Wisconsin Biotechnology Center). Both Illumina libraries were sequenced for 2 × 100 cycles using the Illumina HiSeq2000 system. Strains selected for genome sequencing are indicated in Supporting Information, Table S1.

Genome assembly and annotation of MAT scaffolds

To optimize downstream analyses, a quality control preprocessing step of the raw Illumina data was performed using Trimmomatic v0.32 (Bolger *et al.* 2014). In short, adapter contaminants were clipped and low-quality bases were trimmed at the ends of the reads and when the average quality was below a defined quality threshold (Phred score < 20, using a sliding-window approach). Assembly of both paired-end and mate-pair Illumina reads was carried out using the SPAdes assembler (v.3.1) (Bankevich *et al.* 2012) (parameters: "careful" and "k 35,47,57,65"). Genome assembly quality was assessed by the QUAST analysis tool (Gurevich *et al.* 2013), and final statistics are given in Table S2. Scaffolds encompassing putative *MAT* loci were identified by BLAST searches using as a query a list of *S. salmonicolor MAT*-specific genes (Coelho *et al.* 2010, 2011). The retrieved scaffolds were subsequently annotated using a combination of tools, including Maker 2.10 (Holt and Yandell 2011) with RepBase 19.5 (Jurka *et al.* 2005), SNAP, and Augustus trained on *Rhodosporidium toruloides* NP11 model (PRJNA169538). The annotation of the resulting protein-coding sequences was done using the SIMAP database (Arnold *et al.* 2005) as of late May 2014.

Divergence and synteny analyses

To estimate sequence divergence between the two *L. scottii* strains along *MAT*-containing scaffolds, filtered paired-end reads from CBS 5931 (*MAT* A1) were mapped to the draft assembly of strain CBS 5930 (*MAT* A2) and vice versa, using SMALT v.0.7.6 (https://www.sanger.ac.uk/resources/software/smalt/) with default parameters, except that we set the step size of the hashed words to 2 (-k 13 -s 2). Downstream processes, including the conversion of the SAM output file into a sorted BAM file of mapped reads and variant calling, were performed using various utilities of the SAMtools package v.0.1.18 (Li *et al.* 2009). The consensus genotype in the Variant Call Format was then converted to FASTQ format by limiting maximum depth to 200 to avoid overrepresented regions. A FASTA file was then generated, in which bases with quality lower than 20 (equivalent to 99% of accuracy) were masked to lowercase and ambiguous bases were subsequently converted to an "N." Divergence per site (k, with Jukes–Cantor correction) between the two strains was estimated in VariScan v.2.0.3 (Vilella *et al.* 2005) using a sliding-window analysis (width = 500; jump = 50).

Read mapping was used to support the absence of the genes encoding the transcription factor Ste12, a DNA polymerase subunit (*DNAPolX*) and a Cytochrome P450 reductase in the genome of strain CBS 5931. Raw Illumina paired-end reads from strain CBS 5930 were first mapped against the draft genome assembly of CBS 5931 using the BWA aligner v.0.7.12 (Li and Durbin 2009) with the default settings. Unmapped reads were extracted from the resulting BAM file using SAMtools and the "bamtofastq" utility of BEDTools v.2.16.2 (Quinlan and Hall 2010) and subsequently assembled with SPAdes using the above-mentioned parameters. Genes encoding Ste12, CytP450, and DNAPolX were found within the resulting contigs as assessed by BLAST searches, indicating that the corresponding orthologs are missing in the genome of strain CBS 5931. To account for the possibility of gene sequences being highly divergent between the two

strains, which would prevent the correct alignment of the reads in the first place, raw Illumina reads from CBS 5931 were also mapped to the draft assembly of strain CBS 5930 followed by assembly of the pooled unmapped reads. In this case, none of the three genes were identified in the resulting contigs, reaffirming that they are lacking in the CBS 5931 genome.

Synteny conservation between the two *L. scottii* strains in the scaffolds containing *P/R* and *HD* regions was manually assessed based on the predicted annotations. To further compare *L. scottii MAT* regions with the corresponding regions of other Pucciniomycotina species, we first retrieved the genomes of the red yeasts *Rhodotorula graminis* WP1 and *Sporobolomyces* sp. IAM 13481 (JGI) and the anther-smut *M. lychnidis-dioicae* p1A1 Lamole (Broad Institute) from their respective genome databases. Synteny conservation across species was assessed manually based on their current annotations and as confirmed by high-scoring BLASTP hits in GenBank.

Sequence data and phylogenetic analyses

To infer the phylogenetic relationships of the different strains, sequences of the D1/D2 domain of the LSU rRNA and ITS regions (ITS1, 5.8S and ITS2) were aligned with Clustal W software, trimmed, and merged. The phylogenetic tree was inferred by neighbor-joining using the Kimura two-parameter (K2P) model of evolution in MEGA v.6.0 (Tamura *et al.* 2013). Branch supports were determined using 1000 bootstrap replicates. Sequence from *M. lychnidis-dioicae* TUB 012114 (GenBank accession no. DQ366868/AY877416) and *S. salmonicolor* CBS 490 (GenBank accession no. AF070439/AY015434) were used to root the tree.

The deduced protein sequences of the *HD1* and *HD2* genes of *L. scottii* CBS 5930 and CBS 5931 were aligned, and conserved regions were used to design primers to amplify and sequence an ~1.5-kb fragment, encompassing the 5′ end and intergenic regions of these genes in all strains. The obtained nucleotide sequences, as well as the deduced amino acid sequences, were aligned with MUSCLE (Edgar 2004), and sequence similarity was inspected across all sequences and visualized in UGENE v.1.13.0 (Okonechnikov *et al.* 2012). Coiled-coil dimerization motifs and nuclear localization signals were identified in the complete sequences of the HD1 and HD2 proteins from both sequenced strains using, respectively, COILS (Lupas *et al.* 1991) and PSORTII and SeqNLS (Nakai and Horton 1999; Li and Durbin 2009). Homeodomain regions were predicted by comparison to the previously characterized homeodomain proteins in Pfam database, and the helical contents of the N-terminal domains were predicted with Jpred4 (Drozdetskiy *et al.* 2015). PCR reactions and thermal cycling conditions are given in Table S3 and GenBank accession numbers of the novel *HD1/HD2* sequences are listed in Table S1. *MAT*-specific pheromone receptor genes were amplified by PCR as previously described (de Garcia *et al.* 2015).

Strains, mating tests, and microscopy

The complete list of strains studied and relevant information pertaining to them is given in Table S1. Strains were grown on MYP medium at 17°. Sexual compatibility was investigated by pairing 2- to 4-day-old cultures on Corn Meal Agar (CMA) (Difco), incubated at 17° for 1 week and examined microscopically using phase-contrast optics for production of mycelium and teliospores (globose and thick-walled resting structures that are the site of karyogamy). These tests were carried out two times for each pair of strains and are summarized in Table S4. Production of mycelium and teliospores was classified as extensive when these structure covered all the area of the mating plate (+++), moderate when restricted to a few areas of the plate (++), and poor when these structures were detected only in a single section and took longer time to form (+).

Microscopic observations were made using a Leica DMR microscope equipped with brightfield and differential interference contrast optics, and microphotographs were recorded using a Leica DFC320 digital camera. For fluorescence microscopy, hyphae and vegetative cells from parental crosses or self-fertile (presumably diploid) progeny were submerged into a fixing solution (4% formaldehyde) for 20 min to permeabilize fungal tissue for subsequent staining of nucleic acids with 4',6-diamidino-2-phenylindole. Slides were then observed on an epifluorescence microscopy unit, composed of a Leica DMRA2 Upright Microscope and a CoolSNAP HQ camera. Fluorescence and differential interference contrast acquisitions of Z-series with 0.5-μm increments were performed. Images were processed using ImageJ or Photoshop CS5, and the plug-in straighten was used to straighten curved mycelium (Figure S5A, CBS5931 × 5930 image).

Micromanipulation of teliospores, segregation analysis, and mitotic passages

Strains CBS 5931 and CBS 5930 were mixed on CMA and incubated at 17° for 2 weeks to allow for abundant production of teliospores. Small (~0.5 cm) agar blocks containing teliospores were soaked in sterile distilled water for 4–8 weeks at 4°. After this resting period, a suspension of teliospores was obtained by gently mashing the agar blocks with a small pestle, and this suspension was streaked on the surface of 2% water–agar plates kept at room temperature, using an inoculation loop. Teliospore germination occurred within a week. Using a micromanipulator, basidiospores were individually transferred to a separate section of the plate and allowed to grow for a few days to form a small colony. In cases where germination of the teliospores occurred during the night period, a colony would arise because of the rapid division of the basidiospore initials. In these situations, a variable number of sporidia were separated that could represent either different meiotic products or mitotic daughter cells derived from the basidiospore that first developed. The single-cell-derived colonies were then subcultured onto new MYP plates and stored at −80°. A complete list of the meiotic progeny obtained from this cross is presented in Table S5.

Of the apparently nonhaploid progeny, the *MAT* genotype and associated mating behavior of six single-cell-derived strains was assessed after five consecutive passages in both

yeast extract–peptone–dextrose agar (YPD) and CMA media. Mitotic passages consisted of streaking a few cells onto fresh YPD or CMA plates using a sterile toothpick and growth at 17° for 4 days. In each passage, one-half of the culture plate was used for DNA extraction and storage, while the other half was inspected for the production of teliospores after additional growth in the same conditions. Segregation of the two *MAT* loci in haploid and nonhaploid progeny was assessed by diagnostic PCR with specific primers for the alternate pheromone receptor genes, while *HD1/HD2* alleles were discriminated after PCR amplification by digestion with restriction enzyme *Rsa*I. The primer list and PCR conditions are given in Table S3.

Pulsed-field gel electrophoresis and chromoblots

To isolate chromosomal DNA, cells in stationary phase were harvested by centrifugation. Approximately 2.2×10^9 cells were resuspended in 10 ml of 0.05 M EDTA (pH 8.0), centrifuged (10 min, 5000 × *g*, 4°), and transferred to a pretreatment solution (0.01 M EDTA, 0.1 M Tris–HCl, 0.1 M β-mercaptoethanol, pH 7.4), followed by incubation at 30° for 30 min. After centrifugation, cells were washed twice with 1.2 M sorbitol and resuspended in 500 μl of spheroplasting solution (1.2 M sorbitol, 3 mM EDTA, 0.03 M citric acid, 0.03 M tri-sodium citrate and freshly prepared 10 mg/ml of lysing enzymes from *Trichoderma harzianum*; Sigma-Aldrich, #L1412). This cell suspension was added to 500 μl of 2% low-melting-point agarose, which was premelted in spheroplasting solution without the lytic enzyme and equilibrated at 50° until use. The cell:agarose suspension was mixed and immediately transferred into plug molds (~80 μl each; Bio-Rad, #170-3731) and cooled at 4° for 20 min. Solidified plugs were transferred to 1 ml of spheroplasting solution, incubated at 37° for 2–3 hr, and lysed at 50° for 24 hr in 1 ml of lysing solution (0.01 M Tris–HCl, 0.5 M EDTA, 1% SDS, 1 mg/ml Proteinase K). The lysing step was repeated for 24 hr in refreshed lysing solution. Plugs were finally washed twice with several volumes of 0.05 M EDTA (pH 8.0) and stored at 4° in the same solution until use. To separate chromosomes, plugs were inserted into the wells of an 0.8%-Mb agarose (Bio-Rad, #161-3109) gel prepared in 1× TAE and loaded onto a PFGE apparatus (CHEF DR-III system, Bio-Rad). The electrophoresis was performed at 14° in 1× TAE buffer using the following running conditions: block 1—20 hr, 100–200 sec switch time, 4 V/cm, 120° reorientation angle; block 2—34 hr, 200–400 sec switch time, 3.5 V/cm, 120° angle. The gel was stained in ethidium bromide (1 μg/ml) for 30 min, immediately radiated with 60 mJ of energy in a UV cross-linker (Stratalinker 1800, Stratagene), destained for 30 min, and visualized/photographed under a UV lamp. DNA was denatured for 30 min in several volumes of denaturation buffer (0.5 N NaOH; 1.5 M NaCl) followed by neutralization for 30 min in several volumes of neutralization buffer (1.5 M NaCl, 0.5 M Tris–HCl, pH 7.5) and blotted overnight onto Hybond-N+ membranes (GE Heathcare Life Sciences; #RPN303B) in 20× SSC (0.3 M tri-sodium citrate, 3 M NaCl, pH 7.0–8.0), using standard protocols. The DNA transferred to the membrane was immobilized by UV cross-linking (70 mJ) followed by rinsing in 2× SSC. The membrane was then hybridized with *MAT* gene probes generated by PCR as indicated in Table S3 and labeled with [α-^{32}P] dATP using the Prime-a-Gene Labeling system (Promega, #U1100). Standard protocols were used for hybridization and washing steps. Radioactive signals were detected on X-ray films (Hyperfilm MP, GE Heathcare Life Sciences, #28-9068-50).

Data availability

Scaffolds containing P/R and HD genes from the two newly generated genome sequences were submitted to DNA Data Bank of Japan/European Nucleotide Archive/GenBank under the accession nos. LN868506–LN868513.

Results and Discussion

Characterization of the L. scottii MAT loci and comparison with syntenic genomic regions from related species

Previous studies addressing *MAT* gene content and organization in Pucciniomycotina yeasts suggested that mating type-determining regions of these species might encompass a relatively large portion of a chromosome (Coelho *et al.* 2010; Petit *et al.* 2012; Hood *et al.* 2013; Fontanillas *et al.* 2014; Whittle *et al.* 2015). We therefore considered that defining *MAT* regions in *L. scottii* would benefit from obtaining genome sequences of two strains of compatible mating types since, unlike the rest of the genome, *MAT* loci should be clearly distinct in what concerns sequence divergence and gene organization.

Illumina sequencing of strains CBS 5931 (*MAT* A1) and CBS 5930 (*MAT* A2) resulted in 26.9 Mb of sequence data assembled into 921 and 828 scaffolds, respectively (Table S2). A single receptor gene (*STE3*-like) and three putative pheromone precursor genes presenting the characteristic C-terminal CAAX domain typical of fungal mating pheromones (Coelho *et al.* 2008; Kües *et al.* 2011), localized to a 238-kb-long scaffold (numbered 28; Figure 1) in CBS 5931, as identified by BLAST searches (see *Material and Methods*). A subsequent inspection of this genomic region revealed the presence of other genes previously shown to be involved in mating or required for the onset of the filamentous phase in dimorphic species (*viz. STE20*, Figure 1A) (Nichols *et al.* 2004; Smith *et al.* 2004; Koh *et al.* 2014), in addition to other genes not obviously involved in mating (*e.g.*, *RibL6*, *RibL18*, *RPAC1*, *LSM7*, *MRD1*, and *KAP95*). As for *L. scottii* CBS 5930, homologs of the same set of genes were identified on four different scaffolds (numbered 20, 84, 139 and 151; Figure 1A). Comparison of the two sets of scaffolds from both strains revealed long blocks of conserved synteny flanking a region that exhibited extensive genomic rearrangements. This region, of ~40 kb in CBS 5931 and at least 49 kb in CBS 5930, includes *MAT* A1 and *MAT*

A2-specific pheromone (*RHA*) and receptor (*STE3*) genes and presumably defines the core *P/R* (A) locus in *L. scottii* (Figure 1, highlighted in yellow). Loss of synteny in this region owing to extensive gene rearrangements has likely reduced or suppressed recombination over time, as observed for many other species (Fraser and Heitman 2004, 2005). This configuration is expected to maintain linkage between mating-type-determining genes to prevent the generation of meiotic offspring with self-compatible combinations of pheromones and receptors. A complete synteny recovery can be observed outside the left and right boundaries of the *P/R* locus defined by the genes encoding the PP1/PP2Ac and Prefoldin 3 proteins, respectively (Figure 1).

It is currently recognized that pheromone receptor alleles in both Microbotryales and Sporidiobolales have been anciently recruited to the *P/R* locus and maintained across speciation by balancing selection (Devier *et al.* 2009; Coelho *et al.* 2010). Recent phylogenetic analysis of *L. scottii P/R* alleles revealed that the same holds true: the *STE3.A1* allele sequences were all more similar to the same allele specificity from the distantly related red yeast species than to the alternate conspecific allele (*STE3.A2*) (de Garcia *et al.* 2015). Therefore, genes linked to the *P/R* locus in both mating types are expected to have diverged from each other more significantly than genes unlinked to *MAT*. A sliding-window analysis comparing sequence divergence (k) between the two mating types along the *P/R* locus and neighboring regions indeed shows a general decrease in divergence extending outward from the *P/R* locus (Figure S1). However, for a few allele pairs within the *P/R* locus, sequence divergence is relatively low, indicating that events such as gene conversion (*i.e.*, the unidirectional transfer of allelic sequence) may have contributed to sequence homogenization. In support of this, recent studies have confirmed that gene conversion occurs within the *MAT* locus of two phylogenetically unrelated species: the human fungal pathogen *C. neoformans* (Sun *et al.* 2012) and the unicellular volvocine algae *Chlamydomonas reinhardtii* (De Hoff *et al.* 2013). Gene conversion may therefore be a more broadly occurring phenomenon operating in nonrecombining regions, counteracting to some extent the accumulation of mating-type-linked deleterious mutations that would threaten these regions with gradual deterioration. Remarkably, in *L. scottii* CBS 5930 (*MAT* A2), three genes located at the putative *P/R* locus encoding the transcription factor Ste12, a DNA polymerase subunit (*DNAPolX*), and a Cytochrome P450 reductase do not seem to have an allelic counterpart in any genomic region of the *MAT A1* strain (Figure 1 and Figure S1). These results were further supported by reciprocally mapping of raw Illumina paired-end reads of each *L. scottii* strain against the draft assembly of the other strain. Subsequent assembly of the pooled fraction of unmapped reads and inspection of the gene content by BLAST searches fully corroborated the absence of the three genes in the *MAT* A1 strain. This raises the hypothesis that these genes were lost during evolution as a consequence of gross genomic rearrangements at the *P/R* locus. Of the three genes, only *STE12* is expected to have a mating-related role in *L. scottii* since homologs of this gene were shown to function as master regulators of the pheromone/receptor-signaling pathway in other fungal species (Sprague and Thorner 1992; Zarnack *et al.* 2008; Jones and Bennett 2011). In *C. neoformans*, *C. amylolentus*, and *K. mangrovensis*, *STE12* alleles are mating-type-specific (Findley *et al.* 2009; Guerreiro *et al.* 2013) and, in the former species, this gene is involved in morphogenesis, virulence, and ecological fitness (Chang *et al.* 2001). The presence of *STE12* in only one mating type in *L. scottii* could suggest that it may specifically function during postmating development, but this finding is also consistent with previous observations in the red yeast *R. toruloides* that the initiation of the conjugation tube formation occurs earlier and to a greater extent in cells of one of the mating types (Abe *et al.* 1975). Understanding the function and pattern of evolution of this gene will require a more extensive survey in future studies.

We next compared the genetic organization of the *L. scottii P/R* locus with the homologous regions of the most closely related species for which genome sequencing data were available, *i.e.*, the red yeasts *Sporobolomyces* sp. IAM 13481 (*MAT A1*) and *R. graminis* WP1 (*MAT A2*) and also the anther-smut *M. lychnidis-dioicae* p1A1 Lamole (*MAT A1*). This analysis revealed a considerable conservation in gene content over an ~85-kb stretch of DNA and across species (Figure 1A). In *M. lychnidis-dioicae*, these genes, however, were scattered over several scaffolds, most of which harbored transposable elements at their ends that presumably hampered further assembly (Figure 1A) (Petit *et al.* 2012). Also in *L. scottii* CBS 5930 (*MAT A2*), the core *P/R* locus could not be assembled to such a great extent as the *P/R* A1 locus, even when using a long-range PCR approach to try to close assembly gaps (data not shown). Therefore, we deem it likely that also in this case these regions might be enriched in long repeated sequences and/or transposable elements (Figure 1A). Despite some gene content conservation, some syntenic blocks at the *P/R* locus of *L. scottii* were translocated or inverted compared to the other species. A striking example of this are the gene modules *LSM7-KAP95-STE20* and *RPAC1-RibL6*, which are invariably bordering the *STE3.A2* pheromone receptor gene in several red yeast species (Figure 1A) (Coelho *et al.* 2011). In CBS 5930, the *LSM7-KAP95-STE20* module appears at the left border of the *P/R* locus, whereas two genes usually located at the periphery (*ASF1* and *APO*) are positioned next to the *STE3.A2* gene. This indicates that an inversion has occurred within the *P/R* locus of this mating type followed by additional rearrangements. In addition transposable elements that greatly stimulate intrachromosomal recombination (Fraser *et al.* 2004; Croll *et al.* 2013; Grandaubert *et al.* 2014), another possibility in this case is that such events may have been triggered by the presence of identical and divergently transcribed pheromone precursor genes (*RHA*), which are anchored at the *P/R* locus to constitute large inverted repeats (Figure 1A).

Finally, it is also relevant to mention that we found no evidence in the extant *P/R* locus organization that could support the possibility raised by Fell and Statzell-Tallman concerning the existence of more than two pheromone/receptor

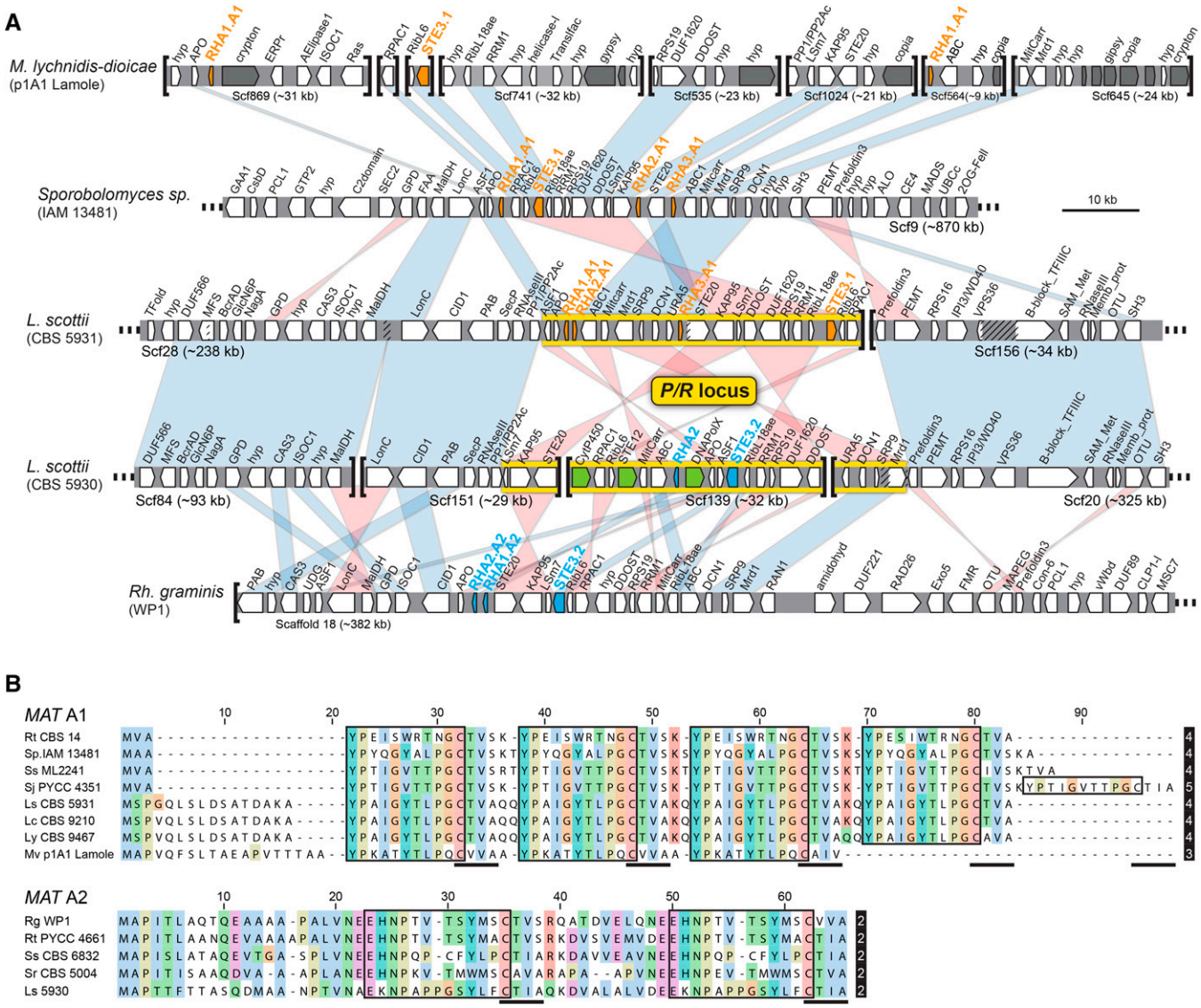

Figure 1 Gene content and organization of the *P/R MAT* locus in *L. scottii* and related species. (A) Structure of the *P/R* locus in strains CBS 5931 (*P/R* A1) and CBS 5930 (*P/R* A2) is shown, along with the corresponding regions from other Pucciniomycotina species. Genes are depicted as arrows denoting the direction of transcription. Vertical blue bars connect orthologs that are in the same orientation, while pink bars indicate inversions. *MAT A1*- and *MAT A2*-specific genes are colored in orange and blue, respectively, in each species. The occurrence of various genomic rearrangements between the two *L. scottii* strains attests to the span of their putative *P/R* loci (highlighted by yellow boxes). The end of a scaffold is indicated by a bracket, and intrascaffold gaps are represented as diagonal stripes. Genes exclusively present at the *P/R* A2 locus of *L. scottii* are shown in green, while those in dark gray represent transposable elements or their remnants. The relative order and the orientations of the *M. lychnidis-dioicae* scaffolds are unknown. (B) Sequence alignment of *MAT* A1 and A2 pheromone precursors from different Pucciniomycotina species (Rt, *R. toruloides*; Rg, *R. graminis*; Sp, *Sporobolomyces* sp.; Ss, *S. salmonicolor*; Sj, *Sporodiobolus johnsonii*, Sr, *Sporodiobolus ruineniae*; Ls, *L. scottii*, Lc, *L. creatinivorum*, Ly, *L. yakuticum*; Mv, *M. lychnidis-dioicae*). Sequence repeats proposed to represent the peptide moiety of the mature pheromone are outlined by a box, while those resembling the CAAX motifs are underlined.

specificities in *L. scottii* (Fell and Statzell-Tallman 1982). First, no evidence was found for the existence of a *P/R* locus consisting of multiple subloci, each encompassing different *P/R* alleles that would freely recombine to generate multiple "A-factors" (Fell and Statzell-Tallman 1982). Second, within the same strain, pheromone precursor genes code for identical peptides, suggesting the presence of only one *MAT* specificity per strain. This organization contrasts, for example, with the triallelic *P/R* locus of several smut species in the Ustilaginales, in which two different *MAT*-specific pheromones are encoded at each *P/R* allele (Schirawski *et al.* 2005; Kellner *et al.* 2011). It also differs from other model species in the subphylum Agaricomycotina, such as *Schizophyllum commune* and *C. cinerea*, in that these species have evolved an enormous repertoire of pheromone/receptor alleles likely arising by duplication of an archetypal *P/R* locus, followed by rounds of recombination and diversification between alleles (Riquelme *et al.* 2005). Other Pucciniomycotina species with complex life

cycles, such as the rust fungi *Puccinia graminis* f. sp. *tritici* and *Melampsora larici-populina*, also seem to encode multiple pheromones and receptors (Duplessis *et al.* 2011; Kües *et al.* 2011) in their genomes, but it is currently unclear whether these predicted genes have a role in determining sexual identity.

Genes encoding the HD1 and HD2 homeodomain transcription factors are always part of the *HD* locus ("B" locus) in basidiomycetes and control postmating development (Kües *et al.* 2011). In *L. scottii*, two divergently transcribed homeodomain homologs (*HD1/HD2*) were identified in a 182-kb-long scaffold in the case of CBS 5931 and in a scaffold of ~492 kb in CBS 5930 (Figure 2). In both cases, these scaffolds are different from those carrying the pheromone/receptor genes. Inspection of the putative *HD* loci from both *L. scottii* strains and comparison with the homologous regions from the same set of species revealed very little gene conservation (Figure 2A). Whereas synteny around the two divergently transcribed *HD1* and *HD2* genes is generally conserved between the two *L. scottii* strains, only a few genes are shared with the two red yeasts species (*e.g.*, *MitCarr*, *PectL*, and *40SRP*) and apparently none with *Microbotryum*; but in the latter species, the *HD*-harboring contig is very small (Figure 2A). When trying to define the boundaries of the *HD* locus in *L. scottii*, we observed that at least two ORFs present in CBS 5931 are absent in CBS 5931, in addition to differences in length of several intergenic regions (Figure 2A). Furthermore, a region spanning ~80 kb and encompassing the *HD1/HD2* genes exhibited increased sequence divergence between the two *L. scottii* strains (Figure 2B) compared to their surrounding genomic regions. These observations are consistent with the possibility that this region of higher sequence divergence may be under (partial) recombination suppression and led us to tentatively place the boundaries of the *L. scottii* core *HD* locus farther apart from the *HD1/HD2* module (Figure 2). Genomic data from additional strains or from a closely related species will be necessary to better support this interpretation.

MAT allele diversity in the L. scottii species complex

Pioneering studies by Fell and Statzell-Tallman addressing sexual incompatibility in *L. scottii* consisted of examining the mating behavior of the progeny of sexual crosses (Fell and Statzell-Tallman 1982). Because this work involved the study of only six natural isolates, we considered that analyzing a wider number of natural isolates would provide a better understanding on *MAT* allele diversity and evolution in this species. Hence, apart from the isolates from this earlier work, we investigated a group of 37 additional strains that represent the phylogenetic diversity of the *L. scottii* species complex (Figure 3 and Table S1). Phylogenetic analyses and mating tests have recently revealed that isolates of the three recognized lineages of this complex (*L. scottii*, *Leucosporidium creatinivorum*, and *Leucosporidium yakuticum*) are very closely related and able to interbreed (de Garcia *et al.* 2015). Interclade crosses, however, seem to be less vigorous than crosses between strains of the same clade (de Garcia *et al.* 2015), thus suggesting that these lineages may be undergoing speciation and that prezygotic barriers are not (yet) present. Our finding that pheromone precursor genes sequenced from representatives of the three *Leucosporidium* clades encode virtually identical peptides, presumably preventing discrimination prior to cell fusion, adds supports this view (Figure 1B).

In Sporidiobolales (red yeasts) and Microbotryales (anther-smuts) only two pheromone receptor alleles exist (*STE3.A1* and *STE3.A2*), and the presence of each allele is always correlated with the mating behavior (Devier *et al.* 2009; Coelho *et al.* 2011). The same holds true for the *L. scottii* species complex (de Garcia *et al.* 2015) (Figure 3A), thus showing that pheromone receptor genes are useful markers of mating-type identity across a broad range of Pucciniomycotina species. Since initial studies suggested that *L. scottii* is a tetrapolar species, we subsequently looked into the distribution and diversity of the *HD1/HD2* alleles (B alleles) and their association with the two pheromone receptors (A alleles). If both loci are located on different chromosomes, as typically observed in tetrapolar species (Bakkeren *et al.* 2006; Findley *et al.* 2012), we should expect a random association between *P/R* and *HD* alleles in natural populations as a result of independent assortment of these alleles during meiosis. To investigate this, we amplified and sequenced a fragment spanning the 5′ end and intergenic regions of the *HD1* and *HD2* genes in 43 strains of the *L. scottii* species complex. This led to the identification of 28 *HD* alleles, all presenting high levels of divergence in the N-terminal domains of both HD1 and HD2 gene products (with 46 and 37% mean identity, respectively) (Figure 3B and Figure S2). Studies involving *C. cinerea* and *U. maydis* HD1 and HD2 proteins showed that this region directs dimerization of proteins from compatible partners (Banham *et al.* 1995; Kämper *et al.* 1995) possibly through coiled-coil interactions. Consistently, similar motifs were also found in the N-terminal domains of *L. scottii* HD1 and HD2 (Figure S2), which strongly suggests that different amino acid sequences in this region are responsible for mating-type specificity.

Allele distribution seems to reflect a progressive sequence diversification during geographic dispersion of *L. scottii* because the extant alleles are clade-specific (Figure 3A). Within the same clade, different *HD* alleles could be recovered from the same geographic region (*e.g.*, alleles B13, B14, B15, B16, and B22 were all found in Portuguese isolates), whereas strains isolated from different locations worldwide could carry the same *HD* allele (*e.g.*, alleles B8 and B6; Figure 3 and Table S1). Despite this, we found no clear evidence of random assortment or recombination between *P/R* and *HD* loci among extant isolates since a particular *HD* allele consistently appears associated with the same receptor allele (*e.g.*, B8, B10, B13, and B17 alleles are always associated with the A1 allele, whereas alleles B2, B6, B22, and B24 co-occur with the A2 allele) (Figure 3A). Such a configuration mirrors the findings in the red yeast *S. salmonicolor*, in which some form of genetic linkage between the two *MAT* loci was proposed

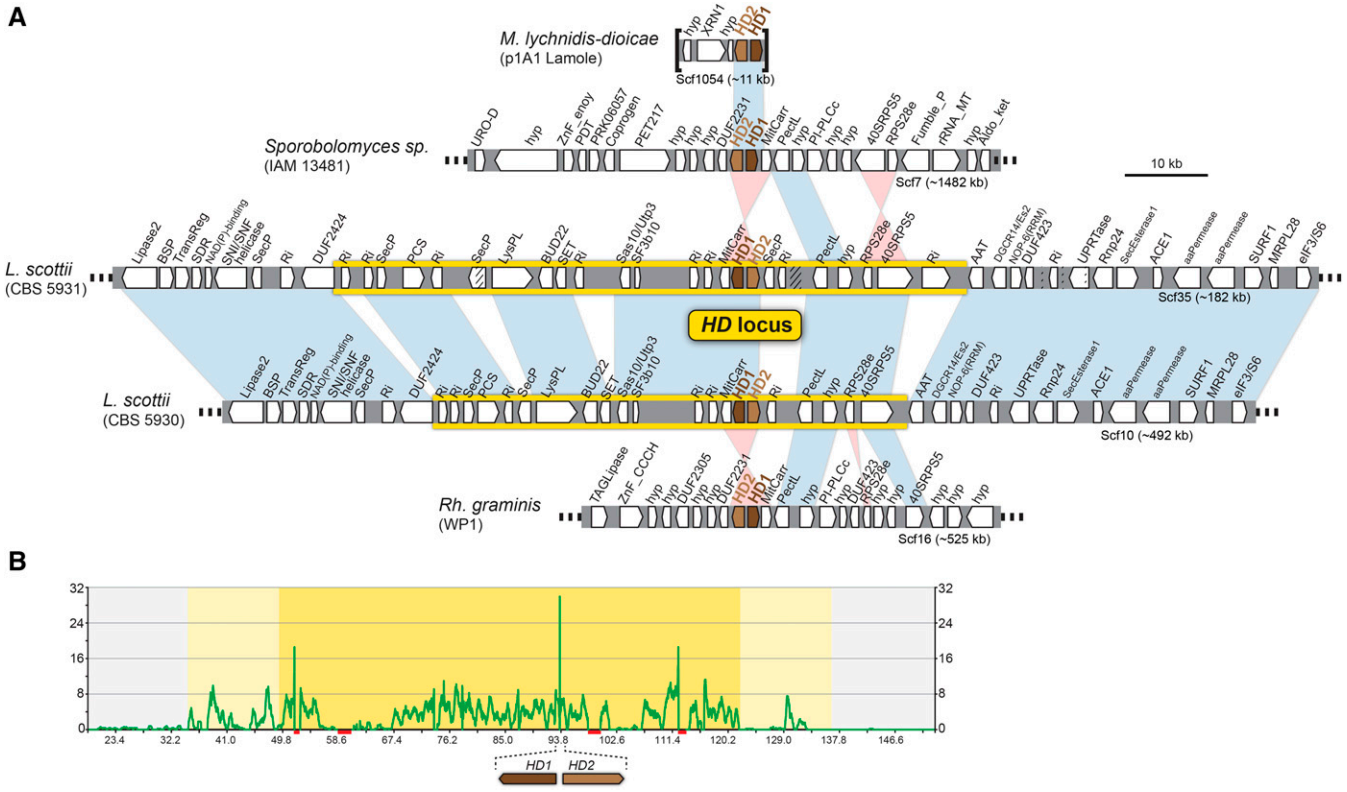

Figure 2 Gene content and organization of the *HD MAT* locus in *L. scottii* and related species. (A) Structure of the *HD* locus in strains CBS 5931 (*HD* B1) and CBS 5930 (*HD* B2) is shown, along with the corresponding regions from other Pucciniomycotina species. The putative *HD* locus (highlighted by yellow boxes) in the two *L. scottii* strains is characterized by the presence of divergently transcribed *HD1* and *HD2* genes (colored in light and dark brown, respectively) and sequence length variation of several intergenic regions (indicated by interruptions in gene synteny). The remaining labels and features are as in Figure 1. (B) Plot representing the percentage of divergence (*k*, with Jukes–Cantor correction; *y*-axis) of CBS 5930 relative to CBS 5931 (*x*-axis values in kilobases) in the genomic regions presented in A. A region of increased divergence comprising the *HD1* and *HD2* genes can be distinguished, in addition to genomic segments that differ between the two strains (these are either absent or too divergent to be aligned; red bars). This region defines the putative *HD* locus (area in yellow). Neighboring regions (light yellow and gray) show a progressive decrease in divergence extending outward from the *HD* locus.

(Coelho *et al.* 2010). However, two intriguing situations were identified for *L. scottii* CBS 9490 and CBS 2300. These strains carry a single *HD* allele (B19 and B23, respectively) and the two *P/R* alleles in the same cell (Figure 3A). While this may suggest that strains are able to undergo mating in nature, such events in some circumstances may generate individuals with apparently unbalanced genotypes at *MAT* (A1A2B19 or A1A2B23). We have also analyzed the molecular mating type of strain CBS 8037, which is a progeny derived from the cross of CBS 5930 (A2B2) and CBS 614 (A1B5) (Fell and Statzell-Tallman 1982). Its mating type was originally designated as *MAT* A3B5 because of its ability to cross with both A1 and A2 strains that do not carry a B5 allele (Fell and Statzell-Tallman 1982). However, our molecular analyses have shown that CBS 8037 is, instead, *MAT* A1A2B5, in agreement with a *P/R* locus that is only biallelic. Together with the observations mentioned above for two wild isolates (CBS 9490 and CBS 2300), these results reaffirm the view that sexual reproduction and meiosis in *L. scottii* may generate offspring with seemingly unbalanced *MAT* genotypes or ploidy variation (diploids or possibly aneuploids), although this does not necessarily lead to sterility. In fact, except for CBS 2300 that only mates as A2, the other two strains were able to mate either as A1 or A2 (Table S4) (de Garcia *et al.* 2015). Nevertheless, the viability or fertility of the progeny resulting from these crosses involving nonhaploid strains remains to be determined.

Finally, additional mating tests for strains, the mating behavior of which had never been tested, showed that with the exception of strain CBS 10581, which is apparently asexual, all strains are fertile (Table S4), even though pairing of sexually competent strains with different alleles at both *MAT* loci did not always yield positive mating reactions (Table S4). Although these results could reflect some form of incompatibility between *HD1/HD2* protein pairs being brought together, the fact that distinct strains with identical mating types do not have completely overlapping mating results (Table S4) suggests that unknown factors and/or genetic background may impose additional barriers to fertility in otherwise compatible mating partners.

Electrophoretic karyotyping and chromosome mapping of P/R and HD loci in L. scottii

The characterization of *L. scottii* sexual progeny (Fell and Statzell-Tallman 1982), the ability to delineate boundaries of *MAT* loci within a relatively short distance from the

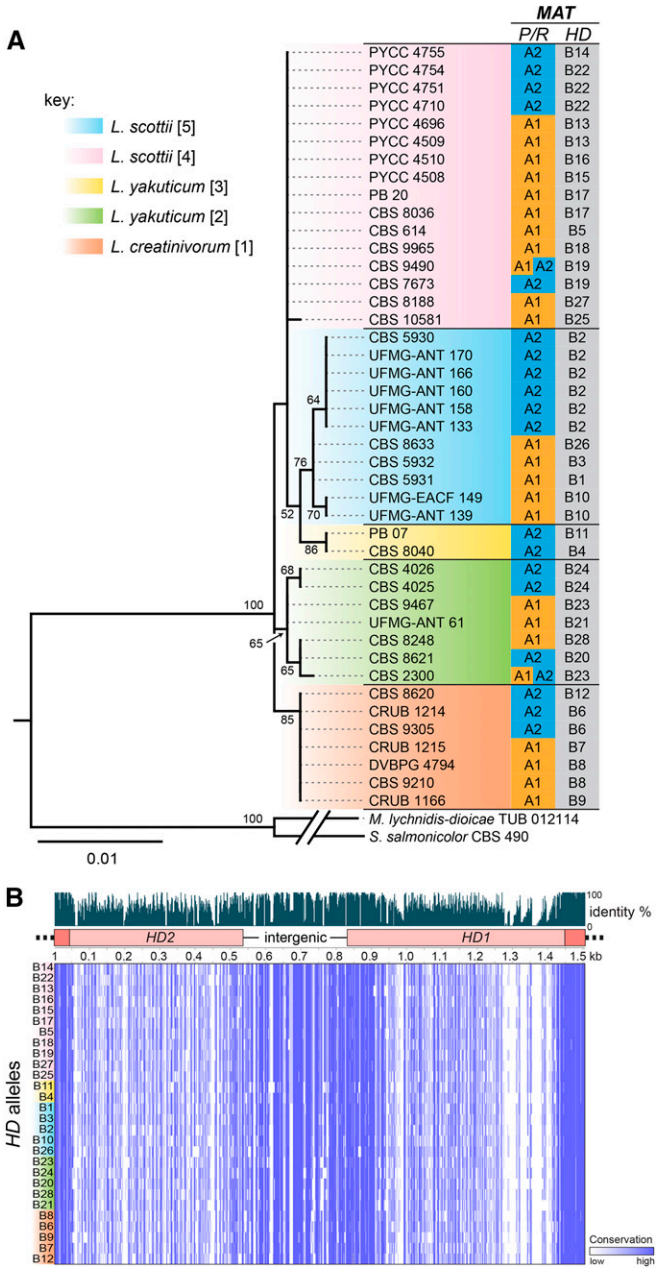

Figure 3 Phylogeny of *L. scottii* species complex and *MAT* allele diversity. (A) Molecular phylogeny representing the major clades of the *L. scottii* species complex (de Garcia *et al.* 2015) as indicated by the color key. The molecular mating type (*MAT*) is given for each of the 43 strains analyzed. With the exception of two apparently nonhaploid strains (CBS 9490 and CBS 2300), a given *HD* allele always appears associated with the same *P/R* allele. The tree was rooted with sequences of *M. lychnidis-dioicae* and *S. salmonicolor*. Bootstrap values (>50%) from 1000 replicates are shown. (B) Nucleotide sequence conservation of *L. scottii HD* alleles, as shown in a percentage identity plot along an ~1.5-kb-long region spanning the homeodomain (dark pink), the variable 5′ end regions (light pink) and common intergenic region of the *HD1* and *HD2* genes. A schematic alignment of the 28 *HD* allele sequences is displayed, with nucleotide positions colored in a blue gradient according to conservation.

MAT-determining genes and also the demonstration of biallelism for the *P/R* locus and multiallelism for the *HD* locus, suggest tetrapolarity in *L. scottii*. To provide unequivocal proof for this, we sought to demonstrate that *P/R* and *HD* loci are physically unlinked. To this end, we used PFGE followed by chromoblot hybridization with specific probes to pinpoint *MAT*-harboring chromosomes of representative strains of the *L. scottii* species complex. This analysis first revealed that strains within the same phylotype generally shared more similar chromosomal band profiles, UFMG-ANT 61 being a noteworthy exception (Figure 4). Although comigrating chromosomal bands hindered the accurate inference of the number of chromosomes, our provisional estimates indicate that strain CBS 5931 harbors 18–20 chromosomes ranging in size from ~0.9 to 2.2 Mb (Figure S3). Two genes were used as probes to identify *MAT* gene-harboring chromosomes: the conserved region of the *HD1* gene was used to localize the *HD* locus whereas for the *P/R* locus we used a fragment of *STE20*, which lies invariably in the immediate vicinity of the receptor genes (Figure 1A). Chromoblot analysis showed that the *HD* locus is located on a higher-molecular-weight chromosome (~1.7 Mb in *L. creatinivorum* and ~1.8–1.9 Mb in *L. scottii* and *L. yakuticum*), while a smaller chromosome harbors the *P/R* locus (~1.25 Mb in all strains) (Figure 4 and Figure S3). The fact that the two *MAT* loci are located on separate chromosomes confirms a tetrapolar mating configuration for the *L. scottii* species complex.

Genotypic analysis of L. scottii meiotic progeny

Assuming that, in nature, sexual reproduction in *L. scottii* follows a random mating pattern, it is intriguing that different allelic combinations of the *P/R* and *HD* genes, imposed by independent assortment of the *MAT* chromosomes, are not detected. Studies with a similar scope on other tetrapolar species (*viz. K. mangrovensis*, *K. heveanensis*, *Cryptococcus flavescens*, and *C. terrestris* (Tremellales, Agaricomycotina) (Metin *et al.* 2010; Guerreiro *et al.* 2013; Yurkov *et al.* 2015) readily detected arbitrary assortment of *MAT* alleles, even within a more restricted number of isolates. Although we cannot rule out that other mechanisms may cause the apparent nonrandom association between *P/R* (A) and *HD* (B) loci in *L. scottii*, we highlight two possibilities in particular. First, a meiotic drive mechanism (Larracuente and Presgraves 2012; Grognet *et al.* 2014) could be in effect, whereby each equal-to-parental pair of *P/R*- and *HD*-harboring chromosomes tend to segregate together. Second, the viability and/or fertility of cells carrying associations of *MAT* alleles reciprocal to those of their parents could be compromised. If so, we then would expect to find in either case a significant bias toward the parental *MAT* genotypes or an altered fertility rate among the offspring. To explore this, we first examined the fate of the parental *MAT* alleles in the F1 progeny derived from a test cross involving *L. scottii* CBS 5931 (A1B1) and CBS 5930 (A2B2). Fell and Statzell-Tallman had already recovered progeny with nonparental *MAT* genotypes (A1B2 and A2B1) from the same parental cross, but the frequency at which this type of progeny occurred was not documented (Fell and Statzell-Tallman 1982). We performed microdissection of 155 randomly collected basidiospores arising from the germination

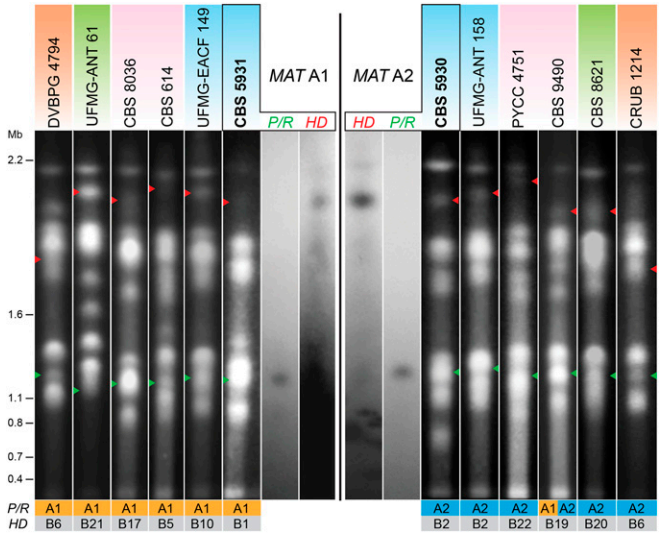

Figure 4 Chromosome mapping of *P/R* and *HD* loci in *L. scottii* species complex. Chromosomes of representative strains of the *L. scottii* species complex were separated using PFGE, followed by chromoblot hybridization with *P/R* and *HD* loci-specific probes (*STE20* and *HD1* genes, respectively). Hybridization signals are shown only for strains CBS 5931 and CBS 5930, which localize the *HD* locus to an ~1.9-Mb chromosome distinct from the localization of the *P/R* locus in an ~1.25-Mb chromosome, as expected in a tetrapolar configuration. Arrowheads indicate chromosome localization of both *MAT* loci for the other strains (red arrows, *HD*; green arrows, *P/R*) (see Figure S3 for details).

of 50 teliospores that represent an equal number of independent meioses. Of these, 135 (87%) viable single-cell-derived cultures were obtained. However, the germination products of a single teliospore also included mitotic descendants likely resulting from the rapid division of the basidiospores that developed first. This was apparent after screening the full set of recovered progeny for the segregation pattern of *MAT* alleles, when more than two sporidia from a single teliospore were of the same mating type (data not shown). Based on this, we selected only 72 meiotic descendants that represented unique meiotic products for further study. About 31% (22/72) of the progeny contained a single *P/R* (A) and *HD* (B) allelic combination (Figure 5). Of these, 64% (14/22) resembled one of the parental strains (A1B1 or A2B2), while reassortment between *P/R* and *HD* loci (*i.e.*, A1B2 and A2B1) was observed in only 36% (8/22) of the cases (Figure 5A). These values, however, do not reflect a significant bias toward a particular combination of *P/R* and *HD* alleles in the progeny (chi-square test, $P > 0.05$). To understand if the haploid progeny with *MAT* recombinant genotypes were as fertile as those with a parental combination of *MAT* alleles, we assessed the outcome of sexual crosses involving representative progeny of each molecular mating type and the tester strains CBS 5931 (A1B1), CBS 5930 (A2B2), CBS 6561 (A1B2), and CBS 6562 (A2B1). Mating tests using a set of 17 progeny revealed that the majority was fertile (Table S6). Only three strains were apparently sterile (#LS053, #LS101, and #LS223), two of which had a parental *MAT* genotype while the other exhibited reassortment between *P/R* and *HD* loci (Table S6). Additional progeny with A1B2 and A2B1 *MAT* genotypes (*e.g.*, #LS118 and #LS090, respectively) were interfertile (Figure 5C and Table S6), but unable to mate when backcrossed with either parental strains (Figure 5C), thus attesting that compatibility at both *MAT* regions is required for heterothallic mating. The remaining progeny (69%; 50/72) were found to be nonhaploid as inferred by the presence of more than one *P/R* or *HD* allele in a single cell (Figure 5A). For example, strains harboring an A1A2B1B2 mating type (*e.g.*, #LS044 and #LS066; Table S5) are apparently diploid since they have inherited both parental *MAT* alleles. These strains produced monokaryotic hyphae with unfused clamp connections and teliospores, which upon germination originated self-sporulating progeny (Figure S4). On the other hand, none of the seemingly nonhaploid progeny that carry both parental *P/R* alleles and only one *HD* allele (*i.e.*, A1A2B1 or A1A2B2) were self-fertile (*e.g.*, #LS072 and #LS025; Figure S5 and Table S6), reaffirming that a single *HD* allele is insufficient to promote sexual reproduction. Conversely, strains with the reciprocal combination of alleles (A1B1B2 or A2B1B2) produced mycelia with teliospores, albeit much less abundantly than the diploid strains, with some teliospores becoming empty after a few weeks (*e.g.*, #LS168 and #LS105; Figure S5 and Table S6). This suggests that the *P/R* system functions essentially as premating determinant, but is still required for normal spore production. Such a situation would parallel the findings reported for *U. maydis*, in which diploid strains homozygous at the *P/R* locus and heterozygous at the *HD* locus (either naturally occurring or genetically transformed with an *HD1/HD2* gene pair of a different allelic specificity) are only able to generate incipient hyphae and teliospores that undergo meiosis and are weakly pathogenic on maize (Banuett and Herskowitz 1989; Bakkeren and Kronstad 1993).

Self-fertile strains have been found among natural isolates of red yeasts of the Sporidiobolales (Sampaio 2011a,b), and their origin may be related with the formation of diploid strains, as earlier studies in the red yeast *R. toruloides* have already suggested (Abe and Sasakuma 1986). The generation of diploid and aneuploid progeny during both unisexual and bisexual reproduction has also been extensively documented in recent studies in *C. neoformans* (Ni *et al.* 2013; Sun *et al.* 2014). Our present observations add support to these studies in that the formation of nonhaploid progeny also seems to be a consistent feature of the life cycle of *L. scottii*. However, it should be noted that, in none of these species are these diploid or aneuploid states prevailing, leading to the presumption that they may represent the outcome of transient solutions triggered under stressful conditions or in specific environmental settings (*e.g.*, nutrient availability) to facilitate rapid adaptive evolution. In line with this, we preliminarily explored in six nonhaploid, single-cell-derived progeny of *L. scottii* whether their *MAT* genotypes and associated mating behavior were maintained with additional subculturing on solid media as a proxy to identify putative ploidy changes. These tests were performed in parallel on both YPD (a high-nutrient medium) and CMA

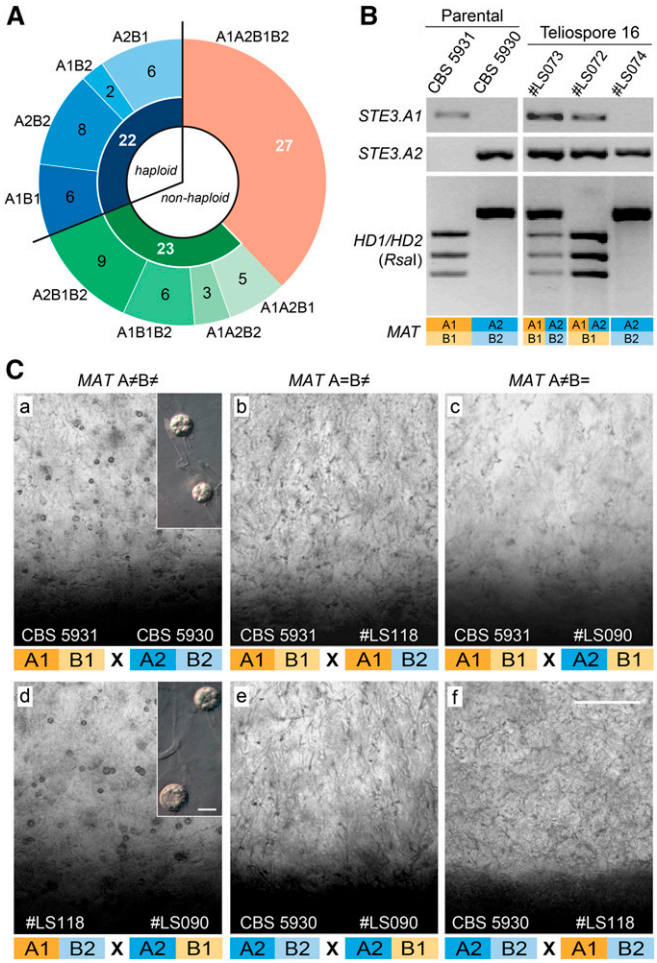

Figure 5 Segregation analysis of *P/R* and *HD* loci and sexual proficiency of CBS 5931 × CBS 5930 progeny. (A) Summary of genotypes at *MAT* of 74 meiotic progeny. (B) An example of the result of the diagnostic PCRs for the presence of the alternate *P/R* alleles (A1 and A2) and discrimination of *HD1/HD2* amplicons by *Rsa*I digestion is shown. Strains #LS073 and #LS072 are apparently nonhaploid. (C) Micrographs of crosses (7 days of incubation on corn meal agar) in all possible combinations between the parental strains (CBS 5931 and CBS 5930) and selected progeny exhibiting nonparental combination of *MAT* alleles (#LS090 and #LS118). The type of cross is indicated in each case. Only in a and d are these crosses able to produce mycelium with teliospores, as shown in higher magnification insets. Bar, 10 μm.

(a low-nutrient, mating-inducing medium) to increase the likelihood of finding changes over time imposed by different nutritional regimes. Interestingly, after five passages, each consisting of transferring a minimal number of cells to induce population bottlenecks, we detected altered mating behavior of the self-fertile strains #LS066 and #LS105 (Figure S5B). Initially characterized as A1A2B1B2 and A2B1B2 (Figure S5B; time point t_1), and producing abundant and limited number of teliospores, respectively, these strains became self-sterile when subcultured on YPD media. Remarkably, this was accompanied by changes in their respective *MAT* genotypes to A1A2B2 and A2B2, as assessed by PCR (Figure S5; time point t_5). Accordingly, *L. scottii* CBS 614 and CBS 5932, which were initially regarded as self-fertile (Fell and Statzell-Tallman 1982), also seem to have lost self-fertility during time possibly due to successive passages in culture media (de Garcia *et al.* 2015). This suggests that these nonhaploid strains are relatively unstable and might undergo a process involving spontaneous chromosome losses to restore the haploid state when selective pressure (in this case sexual cycle-inducing conditions) is relieved, as has been observed in other fungal species (recently reviewed in Forche 2014). Although it is possible that meiosis in *L. scottii* is often inaccurate as part of a stress response mechanism, as stated above, or else due to karyotype variability observed within this species (Figure 4), a more comprehensive study using next-generation sequencing and flow cytometry will be required to address the molecular basis of ploidy transitions and associated phenotypic variation in *L. scottii*. A final hypothesis, which we cannot presently rule out, is that the high numbers of diploid/aneuploid progeny may result from early conjugation of compatible meiotic nuclei still resident in the basidial compartments. Although never documented in *L. scottii*, such intrapromycelial mating has been extensively documented in *M. lychnidis-dioicae* (Hood and Antonovics 1998; Schäfer *et al.* 2010) and seems to be preferred when germination occurs in low-nutrient media.

Taken together, our results indicate that there is no apparent bias in what concerns the viability and fertility of the haploid F1 offspring of *L. scottii*, irrespective of their *MAT* genotype. However, since no clear evidence was gathered for the occurrence of isolates with reassorted *MAT* loci in nature, future studies should address whether or not a similar reproductive fitness is maintained in more distant generations.

Tetrapolarity as the ancestral mating system of basidiomycetes

Transitions in modes of sexual reproduction seem to have continuously occurred over time with most studies highlighting transitions from outcrossing tetrapolar multiallelic systems to bipolar biallelic systems that promote selfing and then to homothallic or unisexual (same-sex) mating. The ancestral state in fungi is likely to be bipolar given the presence of this system in both the Dikarya and Mucoromycotina (Idnurm *et al.* 2008; Heitman *et al.* 2013; Nieuwenhuis *et al.* 2013). A bipolar-to-tetrapolar transition is therefore assumed to have occurred in the Basidiomycota, and genomic footprints suggest that bipolar species within this lineage have evolved secondarily, either by linkage of the two *MAT* loci or due to the loss of the *P/R* locus as an incompatibility determinant (Kües *et al.* 2011; Heitman *et al.* 2013; James *et al.* 2013; Nieuwenhuis *et al.* 2013). However, owing to the occurrence of a myriad of bipolar species within the basidiomycetes, and the paucity of molecular data regarding tetrapolar mating systems in the more basally derived Pucciniomycotina lineage, it has been debatable whether or not tetrapolarity had a single point of origin. Our current findings in the dimorphic yeast *L. scottii* provide valuable insight in this respect. The fact that sexual reproduction in *L. scottii* is dictated by

a tetrapolar mating system, consisting of a biallelic *P/R* locus and a multiallelic *HD* locus, adds further support to tetrapolarity, rather than bipolarity, as the ancestral state of the Basidiomycota. This is the most parsimonious explanation for the co-occurrence of similar tetrapolar configurations in species belonging to the three major lineages of the phylum, as in *Ustilago maydis*, *Kwoniella heveanensis*, and *L. scottii*. Why transitions to bipolarity have occurred multiple times is presently unclear, but for a bipolar system to be selected for, the benefits of a tetrapolar system (namely, increased compatibility owing to multiallelic *MAT* loci and reduced rates of selfing) have likely become less relevant or selected against. In such a scenario, new ecological adaptations with transitions in lifestyles could be either the cause or the consequence of changes in the mating system. The outstanding power of next-generation sequencing, population and comparative genomics, and a broader phylogenetic sampling in the future will allow the understanding of how modes of reproduction (selfing *vs.* outcrossing), mating systems (bipolar *vs.* tetrapolar), and lifestyles (pathogenic *vs.* saprobic) interplay in fungal evolution.

Acknowledgments

We thank Centraalbureau voor Schimmelcultures (The Netherlands), Diego Libkind, and Virginia de Garcia (CRUB, INIBIOMA-CONICET, Argentina) for providing strains and Florent Ubelmann for assistance with epifluorescence microscopy. This work was supported by grant PTDC/BIA-GEN/112799/2009 and project UID/Multi/04378/2013 from Fundação para a Ciência e a Tecnologia, Portugal, and Processes PROANTAR 407230/2013-0 and INCT Criosfera from CNPq. M.A.C. holds a postdoctoral fellowship (SFRH/BPD/79198/2011) from Fundação para a Ciência e a Tecnologia, Portugal. We acknowledge access to the genome sequences of *Sporobolomyces* sp. strain IAM 13481 and *R. graminis* WP1 produced by the U. S. Department of Energy Joint Genome Institute in collaboration with the user community and the *Microbotryum violaceum* Sequencing Project, produced by Broad Institute of MIT and Harvard.

Literature Cited

Abe, K., and T. Sasakuma, 1986 Identification of a diploid self-sporulating cycle in the basidiomycetous yeast *Rhodosporidium toruloides*. J. Gen. Microbiol. 132: 1459–1465.

Abe, K., I. Kusaka, and S. Fukui, 1975 Morphological change in the early stages of the mating process of *Rhodosporidium toruloides*. J. Bacteriol. 122: 710–718.

Aime, M. C., P. B. Matheny, D. A. Henk, E. M. Frieders, R. H. Nilsson *et al.*, 2006 An overview of the higher level classification of Pucciniomycotina based on combined analyses of nuclear large and small subunit rDNA sequences. Mycologia 98: 896–905.

Arnold, R., T. Rattei, P. Tischler, M. D. Truong, V. Stumpflen *et al.*, 2005 SIMAP: the similarity matrix of proteins. Bioinformatics 21(Suppl 2): ii42–ii46.

Badouin, H., M. E. Hood, J. Gouzy, G. Aguileta, S. Siguenza *et al.*, 2015 Chaos of rearrangements in the mating-type chromosomes of the anther-smut fungus *Microbotryum lychnidis-dioicae*. Genetics 200: 1275–1284.

Bakkeren, G., and J. W. Kronstad, 1993 Conservation of the b mating-type gene complex among bipolar and tetrapolar smut fungi. Plant Cell 5: 123–136.

Bakkeren, G., G. Jiang, R. L. Warren, Y. Butterfield, H. Shin *et al.*, 2006 Mating factor linkage and genome evolution in basidiomycetous pathogens of cereals. Fungal Genet. Biol. 43: 655–666.

Bakkeren, G., J. Kämper, and J. Schirawski, 2008 Sex in smut fungi: structure, function and evolution of mating-type complexes. Fungal Genet. Biol. 45(Suppl 1): S15–S21.

Bandoni, R. J., 1963 Conjugation in *Tremella mesenterica*. Can. J. Bot. 41: 467–474.

Banham, A. H., R. N. Asante-Owusu, B. Göttgens, S. Thompson, C. S. Kingsnorth *et al.*, 1995 An N-terminal dimerization domain permits homeodomain proteins to choose compatible partners and initiate sexual development in the mushroom *Coprinus cinereus*. Plant Cell 7: 773–783.

Bankevich, A., S. Nurk, D. Antipov, A. A. Gurevich, M. Dvorkin *et al.*, 2012 SPAdes: a new genome assembly algorithm and its applications to single-cell sequencing. J. Comput. Biol. 19: 455–477.

Banuett, F., and I. Herskowitz, 1989 Different *a* alleles of *Ustilago maydis* are necessary for maintenance of filamentous growth but not for meiosis. Proc. Natl. Acad. Sci. USA 86: 5878–5882.

Billiard, S., M. López-Villavicencio, B. Devier, M. E. Hood, C. Fairhead *et al.*, 2011 Having sex, yes, but with whom? Inferences from fungi on the evolution of anisogamy and mating types. Biol. Rev. Camb. Philos. Soc. 86: 421–442.

Bolger, A. M., M. Lohse, and B. Usadel, 2014 Trimmomatic: a flexible trimmer for Illumina sequence data. Bioinformatics 30: 2114–2120.

Bölker, M., M. Urban, and R. Kahmann, 1992 The *a* mating type locus of *U. maydis* specifies cell signaling components. Cell 68: 441–450.

Casselton, L. A., and U. Kües, 2007 The origin of multiple mating types in the model mushrooms *Coprinopsis cinerea* and *Schizophyllum commune*, pp. 283–300 in *Sex in Fungi: Molecular Determination and Evolutionary Implications*, edited by J. Heitman, J. W. Kronstad, J. W. Taylor, and L. A. Casselton. ASM Press, Washington, D.C.

Chang, Y. C., L. A. Penoyer, and K. J. Kwon-Chung, 2001 The second *STE12* homologue of *Cryptococcus neoformans* is *MAT*a-specific and plays an important role in virulence. Proc. Natl. Acad. Sci. USA 98: 3258–3263.

Coelho, M. A., A. Rosa, N. Rodrigues, Á. Fonseca, and P. Gonçalves, 2008 Identification of mating type genes in the bipolar basidiomycetous yeast *Rhodosporidium toruloides*: first insight into the *MAT* locus structure of the Sporidiobolales. Eukaryot. Cell 7: 1053–1061.

Coelho, M. A., J. P. Sampaio, and P. Gonçalves, 2010 A deviation from the bipolar-tetrapolar mating paradigm in an early diverged basidiomycete. PLoS Genet. 6: e1001052.

Coelho, M. A., P. Goncalves, and J. P. Sampaio, 2011 Evidence for maintenance of sex determinants but not of sexual stages in red yeasts, a group of early diverged basidiomycetes. BMC Evol. Biol. 11: 249.

Croll, D., M. Zala, and B. A. McDonald, 2013 Breakage-fusion-bridge cycles and large insertions contribute to the rapid evolution of accessory chromosomes in a fungal pathogen. PLoS Genet. 9: e1003567.

Dacks, J., and A. J. Roger, 1999 The first sexual lineage and the relevance of facultative sex. J. Mol. Evol. 48: 779–783.

de Garcia, V., M. A. Coelho, T. M. Maia, L. H. Rosa, A. M. Vaz *et al.*, 2015 Sex in the cold: taxonomic reorganization of psychrotolerant yeasts in the order Leucosporidiales. FEMS Yeast Res. 15: pii: fov019.

De Hoff, P. L., P. Ferris, B. J. Olson, A. Miyagi, S. Geng *et al.*, 2013 Species and population level molecular profiling reveals cryptic recombination and emergent asymmetry in the dimorphic mating locus of *C. reinhardtii*. PLoS Genet. 9: e1003724.

Devier, B., G. Aguileta, M. E. Hood, and T. Giraud, 2009 Ancient trans-specific polymorphism at pheromone receptor genes in basidiomycetes. Genetics 181: 209–223.

Drozdetskiy, A., C. Cole, J. Procter, and G. J. Barton, 2015 JPred4: a protein secondary structure prediction server. Nucleic Acids Res. 43: W389–W394.

Duplessis, S., C. A. Cuomo, Y.-C. Lin, A. Aerts, E. Tisserant *et al.*, 2011 Obligate biotrophy features unraveled by the genomic analysis of rust fungi. Proc. Natl. Acad. Sci. USA 108: 9166–9171.

Dyer, P. S., and C. M. O'Gorman, 2012 Sexual development and cryptic sexuality in fungi: insights from *Aspergillus* species. FEMS Microbiol. Rev. 36: 165–192.

Edgar, R. C., 2004 MUSCLE: multiple sequence alignment with high accuracy and high throughput. Nucleic Acids Res. 32: 1792–1797.

Fell, J. W., and A. Statzell-Tallman, 1982 Multiple allelic incompatibility factors among bifactorial strains of the yeast *Leucosporidium* (*Candida*) *scottii*. Curr. Microbiol. 7: 213–215.

Findley, K., M. Rodriguez-Carres, B. Metin, J. Kroiss, Á. Fonseca *et al.*, 2009 Phylogeny and phenotypic characterization of pathogenic *Cryptococcus* species and closely related saprobic taxa in the Tremellales. Eukaryot. Cell 8: 353–361.

Findley, K., S. Sun, J. A. Fraser, Y. P. Hsueh, A. F. Averette *et al.*, 2012 Discovery of a modified tetrapolar sexual cycle in *Cryptococcus amylolentus* and the evolution of MAT in the *Cryptococcus* species complex. PLoS Genet. 8: e1002528.

Fontanillas, E., M. E. Hood, H. Badouin, E. Petit, V. Barbe *et al.*, 2014 Degeneration of the nonrecombining regions in the mating-type chromosomes of the anther-smut fungi. Mol. Biol. Evol. 32: 928–943.

Forche, A., 2014 Large-scale chromosomal changes and associated fitness consequences in pathogenic fungi. Curr. Fungal Infect. Rep. 8: 163–170.

Fraser, J. A., and J. Heitman, 2004 Evolution of fungal sex chromosomes. Mol. Microbiol. 51: 299–306.

Fraser, J. A., and J. Heitman, 2005 Chromosomal sex-determining regions in animals, plants and fungi. Curr. Opin. Genet. Dev. 15: 645–651.

Fraser, J. A., S. Diezmann, R. L. Subaran, A. Allen, K. B. Lengeler *et al.*, 2004 Convergent evolution of chromosomal sex-determining regions in the animal and fungal kingdoms. PLoS Biol. 2: e384.

Gioti, A., B. Nystedt, W. Li, J. Xu, A. Andersson *et al.*, 2013 Genomic insights into the atopic eczema-associated skin commensal yeast *Malassezia sympodialis*. MBio 4: e00572–e00612.

Giraud, T., R. Yockteng, M. López-Villavicencio, G. Refrégier, and M. E. Hood, 2008 Mating system of the anther smut fungus *Microbotryum violaceum*: selfing under heterothallism. Eukaryot. Cell 7: 765–775.

Gonçalves, P., E. Valério, C. Correia, J. M. de Almeida, and J. P. Sampaio, 2011 Evidence for divergent evolution of growth temperature preference in sympatric *Saccharomyces* species. PLoS One 6: e20739.

Goodenough, U., and J. Heitman, 2014 Origins of eukaryotic sexual reproduction. Cold Spring Harb. Perspect. Biol. 6: pii: a016154.

Grandaubert, J., R. G. Lowe, J. L. Soyer, C. L. Schoch, A. P. Van de Wouw *et al.*, 2014 Transposable element-assisted evolution and adaptation to host plant within the *Leptosphaeria maculans-Leptosphaeria biglobosa* species complex of fungal pathogens. BMC Genomics 15: 891.

Grognet, P., H. Lalucque, F. Malagnac, and P. Silar, 2014 Genes that bias Mendelian segregation. PLoS Genet. 10: e1004387.

Guerreiro, M. A., D. J. Springer, J. A. Rodrigues, L. N. Rusche, K. Findley *et al.*, 2013 Molecular and genetic evidence for a tetrapolar mating system in the basidiomycetous yeast *Kwoniella mangrovensis* and two novel sibling species. Eukaryot. Cell 12: 746–760.

Gurevich, A., V. Saveliev, N. Vyahhi, and G. Tesler, 2013 QUAST: quality assessment tool for genome assemblies. Bioinformatics 29: 1072–1075.

Halary, S., S. B. Malik, L. Lildhar, C. H. Slamovits, M. Hijri *et al.*, 2011 Conserved meiotic machinery in *Glomus* spp., a putatively ancient asexual fungal lineage. Genome Biol. Evol. 3: 950–958.

Heitman, J., 2010 Evolution of eukaryotic microbial pathogens via covert sexual reproduction. Cell Host Microbe 8: 86–99.

Heitman, J., S. Sun, and T. Y. James, 2013 Evolution of fungal sexual reproduction. Mycologia 105: 1–27.

Heitman, J., D. A. Carter, P. S. Dyer, and D. R. Soll, 2014 Sexual reproduction of human fungal pathogens. Cold Spring Harb. Perspect. Med. 4: pii: a019281.

Holt, C., and M. Yandell, 2011 MAKER2: an annotation pipeline and genome-database management tool for second-generation genome projects. BMC Bioinformatics 12: 491.

Hood, M. E., 2002 Dimorphic mating-type chromosomes in the fungus *Microbotryum violaceum*. Genetics 160: 457–461.

Hood, M. E., and J. Antonovics, 1998 Two-celled promycelia and mating-type segregation in *Ustilago violacea* (*Microbotryum violaceum*). Int. J. Plant Sci. 159: 199–205.

Hood, M. E., E. Petit, and T. Giraud, 2013 Extensive divergence between mating-type chromosomes of the anther-smut fungus. Genetics 193: 309–315.

Idnurm, A., F. J. Walton, A. Floyd, and J. Heitman, 2008 Identification of the sex genes in an early diverged fungus. Nature 451: 193–196.

James, T. Y., P. Srivilai, U. Kues, and R. Vilgalys, 2006 Evolution of the bipolar mating system of the mushroom *Coprinellus disseminatus* from its tetrapolar ancestors involves loss of mating-type-specific pheromone receptor function. Genetics 172: 1877–1891.

James, T. Y., M. Lee, and L. T. van Diepen, 2011 A single mating-type locus composed of homeodomain genes promotes nuclear migration and heterokaryosis in the white-rot fungus *Phanerochaete chrysosporium*. Eukaryot. Cell 10: 249–261.

James, T. Y., S. Sun, W. Li, J. Heitman, H. C. Kuo *et al.*, 2013 Polyporales genomes reveal the genetic architecture underlying tetrapolar and bipolar mating systems. Mycologia 105: 1374–1390.

Jones, Jr., S. K., and R. J. Bennett, 2011 Fungal mating pheromones: choreographing the dating game. Fungal Genet. Biol. 48: 668–676.

Jurka, J., V. V. Kapitonov, A. Pavlicek, P. Klonowski, O. Kohany *et al.*, 2005 Repbase Update, a database of eukaryotic repetitive elements. Cytogenet. Genome Res. 110: 462–467.

Kämper, J., M. Reichmann, T. Romeis, M. Bölker, and R. Kahmann, 1995 Multiallelic recognition: nonself-dependent dimerization of the bE and bW homeodomain proteins in *Ustilago maydis*. Cell 81: 73–83.

Kellner, R., E. Vollmeister, M. Feldbrugge, and D. Begerow, 2011 Interspecific sex in grass smuts and the genetic diversity of their pheromone-receptor system. PLoS Genet. 7: e1002436.

Koh, C. M., Y. Liu, M. Du Moehninsi, and L. Ji, 2014 Molecular characterization of *KU70* and *KU80* homologues and exploitation of a *KU70*-deficient mutant for improving gene deletion frequency in *Rhodosporidium toruloides*. BMC Microbiol. 14: 50.

Kües, U., T. Y. James, and J. Heitman, 2011 Mating type in Basidiomycetes: unipolar, bipolar, and tetrapolar patterns of

sexuality, pp. 97–160 in *Evolution of Fungi and Fungal-Like Organisms*, edited by S. Pöggeler and J. Wöstemeyer. Springer, Berlin; Heidelberg, Germany; New York.

Larracuente, A. M., and D. C. Presgraves, 2012 The selfish Segregation Distorter gene complex of *Drosophila melanogaster*. Genetics 192: 33–53.

Lawrence, G. J., 1980 Multiple mating-type specificities in the flax rust *Melampsora lini*. Science 209: 501–503.

Li, H., and R. Durbin, 2009 Fast and accurate short read alignment with Burrows–Wheeler transform. Bioinformatics 25: 1754–1760.

Li, H., B. Handsaker, A. Wysoker, T. Fennell, J. Ruan *et al.*, 2009 The Sequence Alignment/Map format and SAMtools. Bioinformatics 25: 2078–2079.

Lupas, A., M. Van Dyke, and J. Stock, 1991 Predicting coiled coils from protein sequences. Science 252: 1162–1164.

Metin, B., K. Findley, and J. Heitman, 2010 The mating type locus (*MAT*) and sexual reproduction of *Cryptococcus heveanensis*: insights into the evolution of sex and sex-determining chromosomal regions in fungi. PLoS Genet. 6: e1000961.

Nadal, M., M. D. García-Pedrajas, and S. E. Gold, 2008 Dimorphism in fungal plant pathogens. FEMS Microbiol. Lett. 284: 127–134.

Nakai, K., and P. Horton, 1999 PSORT: a program for detecting sorting signals in proteins and predicting their subcellular localization. Trends Biochem. Sci. 24: 34–36.

Narisawa, K., Y. Yamaoka, and K. Katsuya, 1994 Mating type of isolates derived from the spermogonial state of *Puccinia coronata* var. *coronata*. Mycoscience 35: 131–135.

Ni, M., M. Feretzaki, W. Li, A. Floyd-Averette, P. Mieczkowski *et al.*, 2013 Unisexual and heterosexual meiotic reproduction generate aneuploidy and phenotypic diversity de novo in the yeast *Cryptococcus neoformans*. PLoS Biol. 11: e1001653.

Nichols, C. B., J. A. Fraser, and J. Heitman, 2004 PAK kinases Ste20 and Pak1 govern cell polarity at different stages of mating in *Cryptococcus neoformans*. Mol. Biol. Cell 15: 4476–4489.

Nieuwenhuis, B. P., S. Billiard, S. Vuilleumier, E. Petit, M. E. Hood *et al.*, 2013 Evolution of uni- and bifactorial sexual compatibility systems in fungi. Heredity (Edinb) 111: 445–455.

Okonechnikov, K., O. Golosova, and M. Fursov; UGENE team, 2012 Unipro UGENE: a unified bioinformatics toolkit. Bioinformatics 28: 1166–1167.

Petit, E., T. Giraud, D. M. de Vienne, M. A. Coelho, G. Aguileta *et al.*, 2012 Linkage to the mating-type locus across the genus *Microbotryum*: insights into nonrecombining chromosomes. Evolution 66: 3519–3533.

Quinlan, A. R., and I. M. Hall, 2010 BEDTools: a flexible suite of utilities for comparing genomic features. Bioinformatics 26: 841–842.

Raper, J. R., 1966 *Genetics of Sexuality in Higher Fungi*. The Roland Press, New York.

Riquelme, M., M. P. Challen, L. A. Casselton, and A. J. Brown, 2005 The origin of multiple *B* mating specificities in *Coprinus cinereus*. Genetics 170: 1105–1119.

Sampaio, J. P., 2011a *Rhodosporidium* Banno, pp. 1523–1540 in *The Yeasts: A Taxonomic Study*, Vol. 3, Part Vb, edited by C. P. Kurtzman, J. W. Fell, and T. Boekhout. Elsevier, Amsterdam.

Sampaio, J. P., 2011b *Sporidiobolus* Nyland, pp. 1549–1562 in *The Yeasts: A Taxonomic Study*, Vol. 3, Part Vb, edited by C. P. Kurtzman, J. W. Fell, and T. Boekhout. Elsevier, Amsterdam.

Sampaio, J. P., M. Gadanho, R. Bauer, and M. Weiss, 2003 Taxonomic studies in the Microbotryomycetidae: *Leucosporidium golubevii* sp. nov., *Leucosporidiella* gen. nov. and the new orders Leucosporidiales and Sporidiobolales. Mycol. Prog. 2: 53–68.

Schäfer, A. M., M. Kemler, R. Bauer, and D. Begerow, 2010 The illustrated life cycle of *Microbotryum* on the host plant *Silene latifolia*. Botany 88: 875–885.

Schirawski, J., B. Heinze, M. Wagenknecht, and R. Kahmann, 2005 Mating type loci of *Sporisorium reilianum*: novel pattern with three *a* and multiple *b* specificities. Eukaryot. Cell 4: 1317–1327.

Smith, D. G., M. D. Garcia-Pedrajas, W. Hong, Z. Yu, S. E. Gold *et al.*, 2004 An *ste20* homologue in *Ustilago maydis* plays a role in mating and pathogenicity. Eukaryot. Cell 3: 180–189.

Sprague, G. F., Jr., and J. W. Thorner, 1992 Pheromone response and signal transduction during the mating process of *Saccharomyces cerevisiae*, pp. 657–744 in *The Molecular and Cellular Biology of the Yeast Saccharomyces*, Vol. 2, *Gene Expression*, edited by J. R. Broach, J. Pringle, and E. W. Jones. Cold Spring Harbor Laboratory Press, Cold Spring Harbor, NY.

Sun, S., Y. P. Hsueh, and J. Heitman, 2012 Gene conversion occurs within the mating-type locus of *Cryptococcus neoformans* during sexual reproduction. PLoS Genet. 8: e1002810.

Sun, S., R. B. Billmyre, P. A. Mieczkowski, and J. Heitman, 2014 Unisexual reproduction drives meiotic recombination and phenotypic and karyotypic plasticity in *Cryptococcus neoformans*. PLoS Genet. 10: e1004849.

Tamura, K., G. Stecher, D. Peterson, A. Filipski, and S. Kumar, 2013 MEGA6: Molecular Evolutionary Genetics Analysis version 6.0. Mol. Biol. Evol. 30: 2725–2729.

Vilella, A. J., A. Blanco-Garcia, S. Hutter, and J. Rozas, 2005 VariScan: analysis of evolutionary patterns from large-scale DNA sequence polymorphism data. Bioinformatics 21: 2791–2793.

Whittle, C. A., A. Votintseva, K. Ridout, and D. A. Filatov, 2015 Recent and massive expansion of the mating-type specific region in the smut fungus *Microbotryum*. Genetics 199: 809–816.

Yamazaki, S., and K. Katsuya, 1988 Mating type of pine gall rust fungus, *Cronartium quercuum*. Proc. Jpn. Acad. 64 Ser. B: 197–200.

Yi, R., T. Tachikawa, M. Ishikawa, H. Mukaiyama, D. Bao *et al.*, 2009 Genomic structure of the *A* mating-type locus in a bipolar basidiomycete, *Pholiota nameko*. Mycol. Res. 113: 240–248.

Yurkov, A., M. A. Guerreiro, L. Sharma, C. Carvalho, and A. Fonseca, 2015 Multigene assessment of the species boundaries and sexual status of the basidiomycetous yeasts *Cryptococcus flavescens* and *C. terrestris* (Tremellales). PLoS One 10: e0120400.

Zarnack, K., H. Eichhorn, R. Kahmann, and M. Feldbrügge, 2008 Pheromone-regulated target genes respond differentially to MAPK phosphorylation of transcription factor Prf1. Mol. Microbiol. 69: 1041–1053.

Communicating editor: J. Heitman

GENETICS

Supporting Information
www.genetics.org/lookup/suppl/doi:10.1534/genetics.115.177717/-/DC1

Evolution of Mating Systems in Basidiomycetes and the Genetic Architecture Underlying Mating-Type Determination in the Yeast *Leucosporidium scottii*

Teresa M. Maia, Susana T. Lopes, João M. G. C. F. Almeida, Luiz H. Rosa, José Paulo Sampaio, Paula Gonçalves, and Marco A. Coelho

DOI: 10.1534/genetics.115.177717

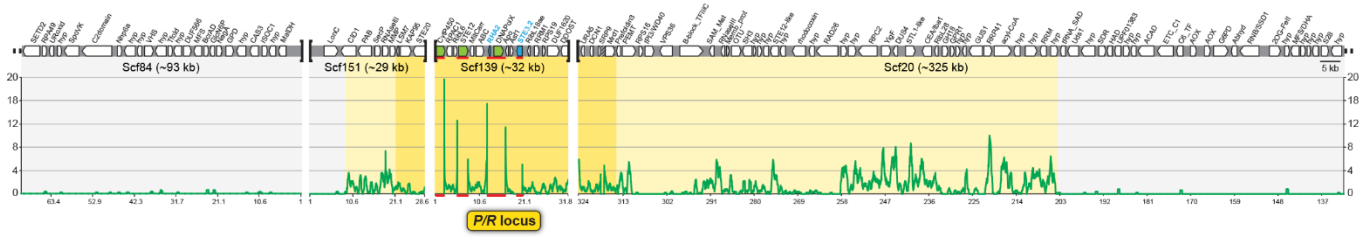

Figure S1 Divergence plot between *MAT* A1 and *MAT* A2 strains of *L. scottii* at the putative *P/R* locus. Sliding window analysis of percentage divergence (*k*, with Jukes-Cantor correction; y-axis) of CBS 5931 relative to CBS 5930 scaffolds (x-axis values in kb) encompassing the putative *P/R* locus and neighboring regions. The *P/R* locus (area in yellow) displays an increased divergence between the two strains and includes genomic segments that are specific of strain CBS 5930 (red bars), for instance, the pheromone (*RHA2*) and pheromone receptor (*STE3.2*) genes, as well as the transcription factor encoding gene *STE12*. Neighboring regions (light yellow and grey) show a general decrease in divergence extending outwards from the core *P/R* locus. The remaining labels and features are as in Figure 1.

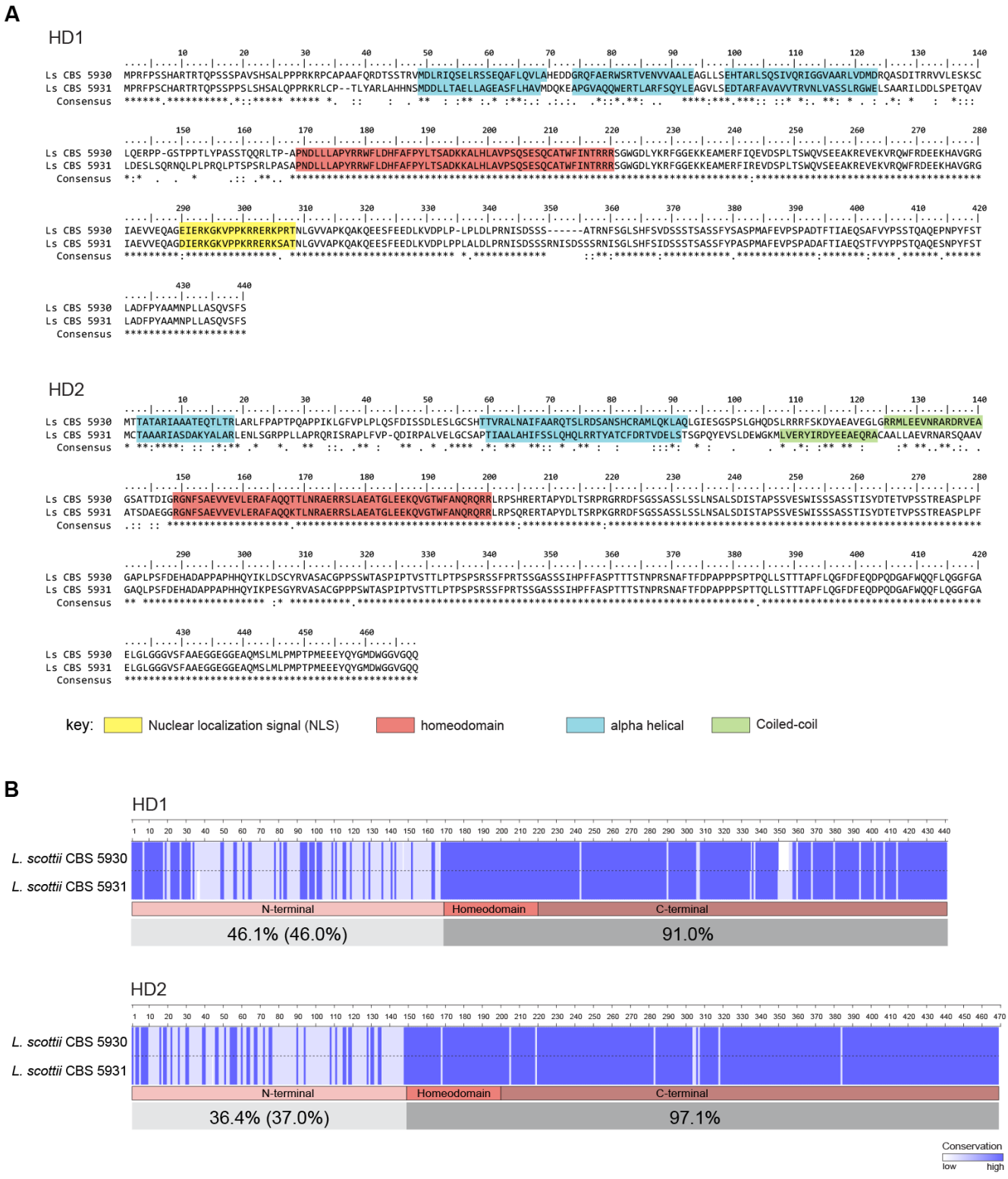

Figure S2 Sequence alignment of the HD1 and HD2 gene products from *L. scottii* strains CBS 5930 and CBS 5931. (A) The HD1 and HD2 amino acid sequences display allele-specific variability in their N-terminal domains while showing a high degree of sequence conservation in the C-terminal domain and homeodomain motif. Typical HD1 and HD2 protein secondary structure features are highlighted according to the key below. (B) Sequence identity between each pair of HD1 and HD2 proteins is given for the variable (N-termini) and conserved (homeodomain and C-termini) regions with amino acid positions colored in a blue gradient according to conservation. Values in brackets in the N-terminal regions are the average identity as calculated from all the 28 different allele products.

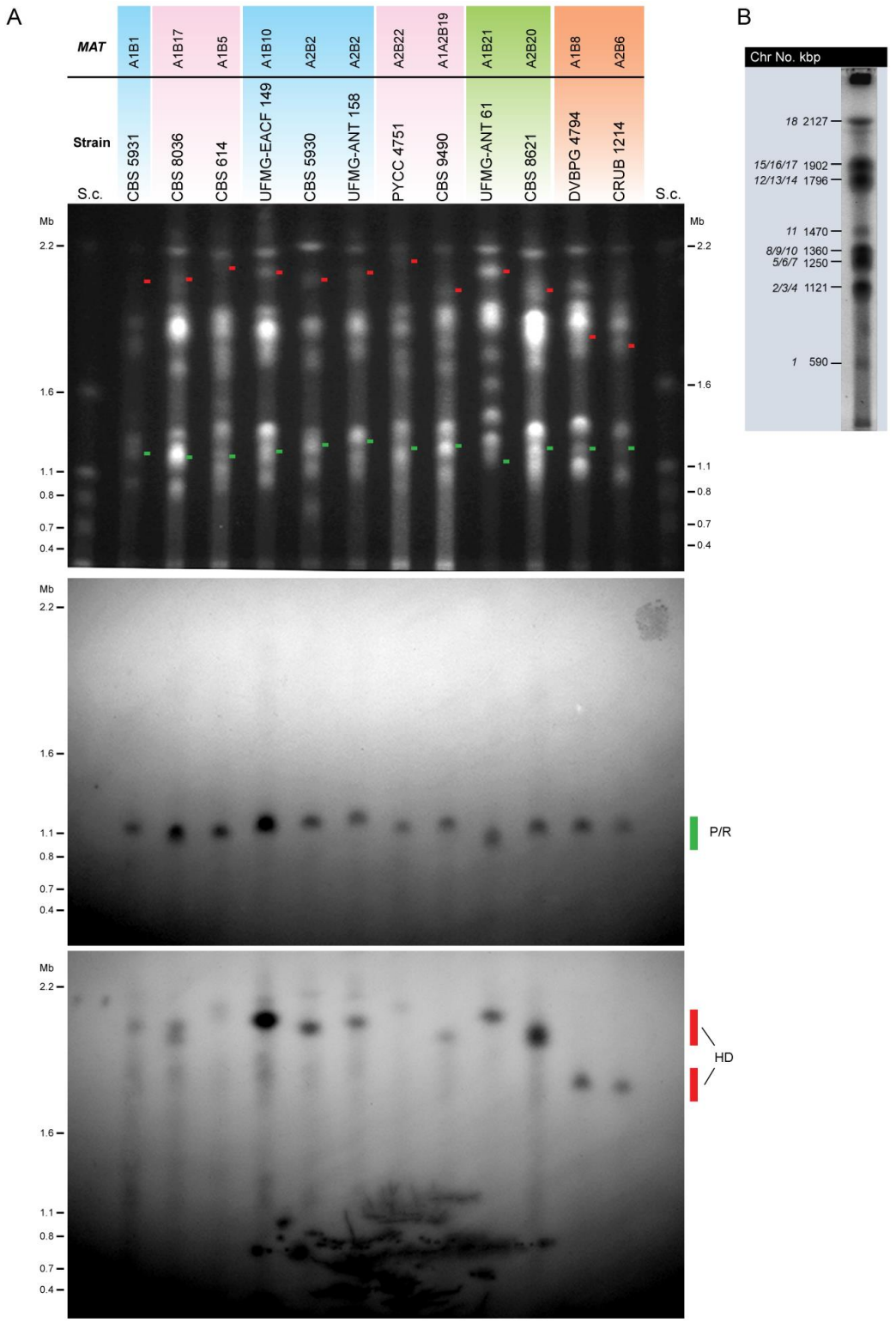

Figure S3 Original electrophoretic karyotypes and localization of *MAT* chromosomes in strains of the *L. scottii* species complex. (A) Raw, uncropped images of the electrophoretic karyotype gel (top section) and hybridization results with *P/R* (middle section) and *HD* (bottom section) probes as outlined in Figure 3. (B) Electrophoretic karyotype of strain CBS 5931 used for chromosome size estimation. The number of chromosomes are indicated along with their approximate size (in kb).

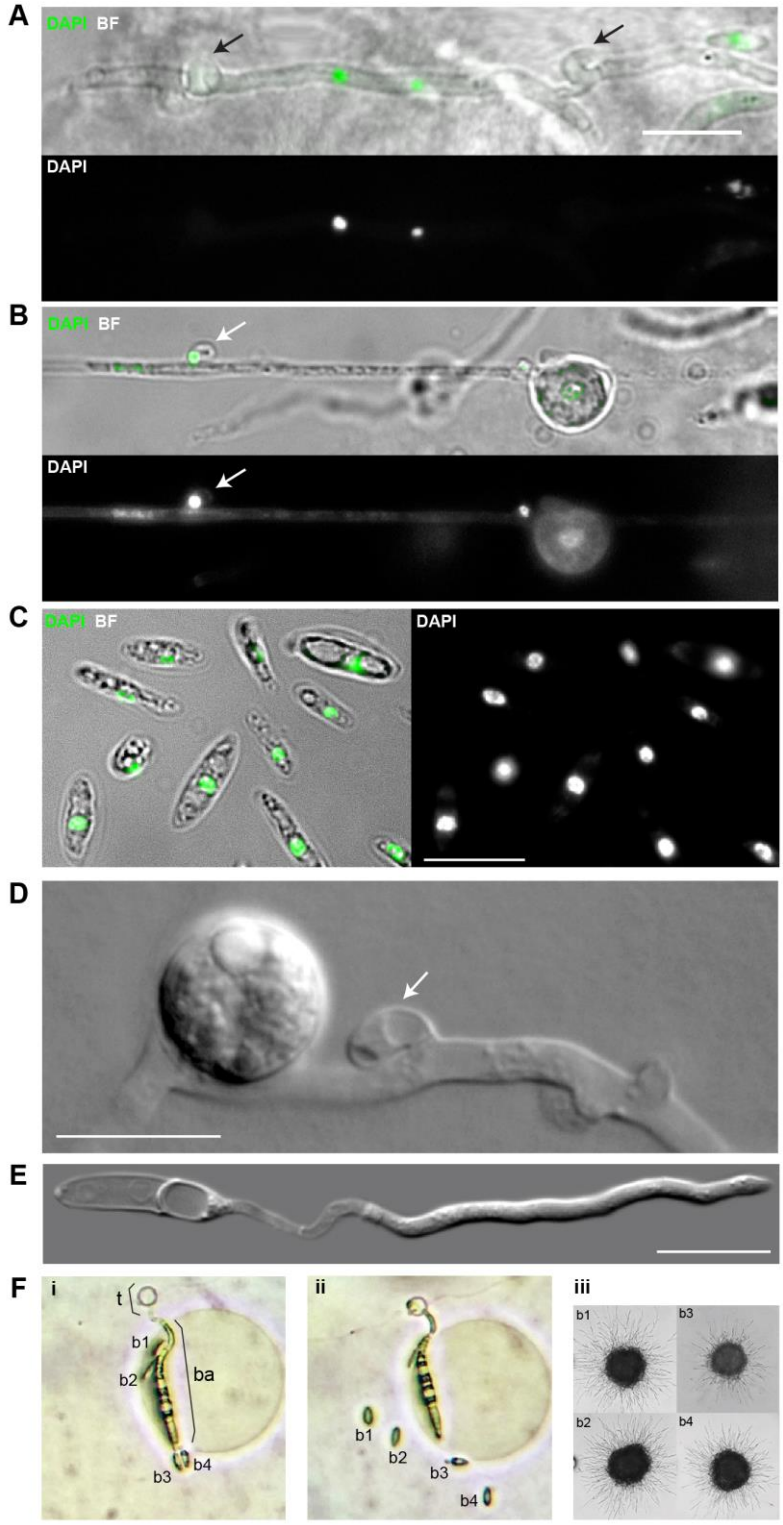

Figure S4 Morphological characterization of the self-fertile strain #LS044. (A) Micrograph from cross CBS 5931 x CBS 5930, in which dikaryotic mycelium can be visualized. Cell boundaries can be perceived on the left, by the presence of an immature teliospore (out-of-focus) and on the right by a clamp connection (black arrows). (B) Micrograph of monokaryotic mycelium adjacent to a teliospore in strain #LS044, showing a nucleus arrested in the unfused clamp connection (white arrow). (C) Uninucleate yeast cells of strain #LS044. In panels (A), (B) and (C), merged Bright-field and DAPI channels are indicated by 'DAPI BF' while DAPI-only channel is indicated by 'DAPI'. (D) Differential Interference Contrast (DIC) micrograph showing in more detail an unfused clamp connection (white arrow) in strain #LS044. (E) DIC micrograph exhibiting the self-filamentation phenotype of strain #LS044. (F) Germinating teliospore of #LS044 is able to produce viable offspring. t: teliospore; ba: basidium; b1, b2, b3, b4: basidiospores 1 to 4. (i) Teliospore at the beginning of germination. (ii) Germinated teliospore next to four basidiospores separated using a micromanipulator. iii. Self-filamentation phenotype of the four recovered spores. Scale bars: 10 µm.

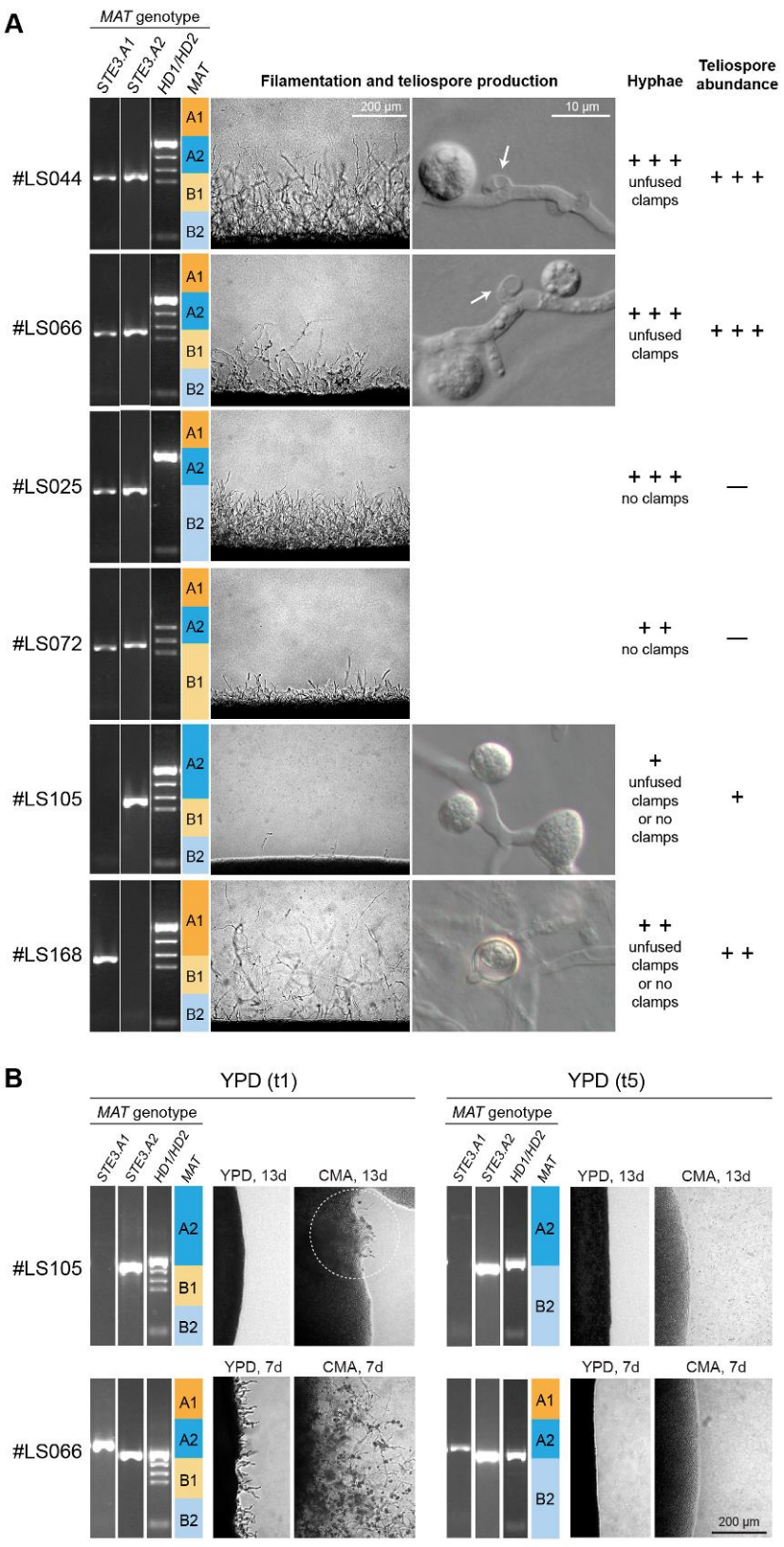

Figure S5 Morphology and sexual behavior of *L. scottii* progeny with unbalanced *MAT* genotypes. (A) Non-haploid progenies derived from the CBS 5930 x CBS 5931. For each strain is shown (from the left to the right) the identification of the *MAT* genotype by PCR/RFLPs, micrographs of mycelium and teliospores produced in CMA medium, type of hyphae and the abundance of teliospores. Strains #LS044 and #LS066 (*MAT* A1A2B1B2) are self-sporulating, establishing hyphae with unfused clamps. Strains #LS025 and #LS072, which carry compatible A alleles and only one B allele, are unable to produce teliospores despite producing extensive hyphae. In contrast, strains that harbor compatible B alleles and only one A allele (#LS105 and #LS168) produce incipient hyphae and teliospores, some of which become empty after a few weeks. (B) Self-sporulating strains have unstable phenotypes and genotypes. Growth in YPD and CMA media of #LS105 and #LS066 cells that had been recovered at passages one (left panel, t1) and five (right panel, t5) of the sub-culturing experiment (successive passages in nutrient-rich YPD medium). These strains underwent a transition to a self-sterile phenotype after five passages as observed by loss of sexual development in CMA medium and concomitant change in their respective *MAT* genotypes.

Table S1 List of *L. scottii* strains used in this study and relevant information pertaining to them.

Strain	Substrate	Location	Species	Phylotype [a]	*MAT* genotype		HD1/HD2 (GenBank)	D1/D2 LSU (GenBank)	ITS region (GenBank)	Fertility
					P/R	*HD*				
CBS 8620^{T}	permafrost soil	Russia	*L. creatinivorum*	1	A2	B12	KR229936	AF189925	AF444629	– [g]
CBS 9210	soil	Iceland	*L. creatinivorum*	1	A2	B8	KR229942	KM213196	KM213169	– [g]
CBS 9305	soil	Russia	*L. creatinivorum*	1	A2	B6	KR229937	EF643737	KM213172	n.a.
CRUB 1166	river	Argentina	*L. creatinivorum*	1	A1	B9	KR229940	EF595758	KM213173	– [g]
CRUB 1214 [f]	river	Argentina	*L. creatinivorum*	1	A2	B6	KR229938	DQ513291	KM213174	+ [g]
CRUB 1215	river	Argentina	*L. creatinivorum*	1	A1	B7	KR229939	KM213199	KM213175	+ [g]
DVBPG 4794 [f]	glacier	Alps	*L. creatinivorum*	1	A1	B8	KR229941	EF643737	KM213170	+ [g]
CBS 2300	air	Norway	*L. yakuticum*	2	A1A2	B23	KR229950	KM213202	KM213178	+ [g]
CBS 4025	soil	Germany	*L. yakuticum*	2	A2	B24	KR229947	KP732295	KP732311	+
CBS 4026	unknown	unknown	*L. yakuticum*	2	A2	B24	KR229948	KP732296	KP732312	+
CBS 8248	water	Antarctica	*L. yakuticum*	2	A2	B28	KR229951	KM213177	KM213201	+ [g]
CBS 8621^{T} [f]	permafrost rock	Russia	*L. yakuticum*	2	A2	B20	KR229945	AY213001	AY212989	+ [g]
CBS 9467	soil	EUA	*L. yakuticum*	2	A1	B23	KR229949	KP732297	KP732313	+ [g]
UFMG-ANT 61 [f]	plant	Antarctica	*L. yakuticum*	2	A1	B21	KR229946	KM213205	KM213180	+ [g]
CBS 8040	water	USA	*L. yakuticum*	3	A2	B4	KR229943	KM213204	KM213179	+ [g]
PB 07	oil-shale mine	Austria	*L. yakuticum*	3	A2	B11	KR229944	KM213203	AJ853458	n.a.
CBS 5930^{T} [e][f]	seawater	Antarctica	*L. scottii*	4	A2	B2	KR229952	AY213000	AF444495	++ [b]
CBS 5931 [e][f]	seawater	Antarctica	*L. scottii*	4	A1	B1	KR229953	KP732310	KM213181	++ [b]
CBS 5932	seawater	Antarctica	*L. scottii*	4	A1	B3	KR229954	AF189908	AF444496	++ [b] [c]
CBS 8633	plant	Russia	*L. scottii*	4	A1	B26	KR229962	DQ531949	KP732326	++
UFMG-ANT 133	water	Antarctica	*L. scottii*	4	A2	B2	KR229961	KM213218	KM213194	++ [g]
UFMG-ANT 139	water	Antarctica	*L. scottii*	4	A1	B10	KR229955	KM213212	KM213188	++ [g]
UFMG-ANT 158 [f]	water	Antarctica	*L. scottii*	4	A2	B2	KR229960	KM213217	KM213193	++ [g]
UFMG-ANT 160	water	Antarctica	*L. scottii*	4	A2	B2	KR229957	KM213216	KM213192	++ [g]
UFMG-ANT 166	water	Antarctica	*L. scottii*	4	A2	B2	KR229958	KM213214	KM213190	++ [g]
UFMG-ANT 170	water	Antarctica	*L. scottii*	4	A2	B2	KR229959	KM213215	KM213191	++ [g]
UFMG-EACF 149 [f]	water	Antarctica	*L. scottii*	4	A1	B10	KR229956	KM213213	KM213189	++ [g]
CBS 10581	soil	New Zealand	*L. scottii*	5	A1	B25	KR229974	KP732298	KP732314	–
CBS 614 [f]	soil	Australia	*L. scottii*	5	A1	B5	KR229973	KM213207	KM213183	++ [b] [c]
CBS 7673	water	unknown	*L. scottii*	5	A2	B19	KR229978	KP732296	KP732315	++ [g]
CBS 8036 [f]	soil	unknown	*L. scottii*	5	A1	B17	KR229971	KP732300	KP732316	++
CBS 8188	seaweed	Canada	*L. scottii*	5	A1	B27	KR229975	KP732302	KP732318	+
CBS 9490 [f]	soil	Netherlands	*L. scottii*	5	A1A2	B19	KR229977	KP732301	KP732317	+
CBS 9965	rotten wood	Netherlands	*L. scottii*	5	A1	B18	KR229976	KM213210	KM213186	+ [d] [g]
PB 20	railway area	Austria	*L. scottii*	5	A1	B17	KR229972	KM213209	KM213185	+ [g]
PYCC 4508	flower	Portugal	*L. scottii*	5	A1	B16	KR229969	KP732303	KP732319	+
PYCC 4509	soil	Portugal	*L. scottii*	5	A1	B15	KR229970	KP732304	KP732320	+
PYCC 4510	leaf	Portugal	*L. scottii*	5	A1	B13	KR229964	KP732305	KP732321	+
PYCC 4696	dry leafs	Portugal	*L. scottii*	5	A1	B13	KR229965	KM213211	KM213187	++
PYCC 4710	river	Portugal	*L. scottii*	5	A1	B13	KR229963	KP732306	KP732322	n.a.
PYCC 4751 [f]	wood	Portugal	*L. scottii*	5	A2	B22	KR229966	KP732307	KP732323	+
PYCC 4754	moss	Portugal	*L. scottii*	5	A2	B22	KR229967	KP732308	KP732324	+
PYCC4755	soil	Portugal	*L. scottii*	5	A2	B14	KR229968	KP732309	KP732325	+

Abbreviations: L., *Leucosporidium*; T, Type strain; CBS, Centraalbureau voor Schimmelcultures, The Netherlands; CRUB, Regional University Center of Bariloche (Centro Regional Universitario Bariloche), Argentina; EXF, Culture Collection of Extremophilic Fungi, University of Ljubljana, Slovenia; UFMG, Minas Gerais Federal University (Universidade Federal de Minas Gerais), Brazil; PYCC, Portuguese Yeast Culture Collection, FCT/UNL, Portugal; DBVPG, Industrial Yeasts Collection, University of Perugia, Italy. (–) apparently infertile (asexual); (+) moderate fertility (formation of sexual structures may take longer and/or be less frequent, or even not occur with fertile strains of compatible molecular mating type); (++) fertile with extensive production of teliospores; n.a., not assessed.

(a) Phylogenetic subclade within *Leucosporidium scottii* species complex, as defined by de Garcia et al. 2015.

(b) Strain fertility has been assessed in various studies including Fell and Statzell-Tallman 1982, de Garcia et al. 2015 and this study.

(c) Strain reported to be self-fertile in Fell and Statzell-Tallman 1982.

(d) Strain reported to be self-fertile in de Garcia et al. 2015.

(e) Strains used for whole-genome sequencing

(f) Strains used in chromoblots analyses

(g) Fertility assessed by de Garcia et al. 2015.

Table S2 Genome sequencing strategy and final genome assembly statistics.

L. scottii strains	Illumina sequencing (Hiseq 2000)										Draft genome assembly statistics					
	Paired-end (PE) libraries					Mate-pair (MP) libraries										
	run (cycles)	insert-size (bp)	# paired reads	Total length (Gb)	Coverage (~ 20 Mb)	run (cycles)	insert-size (bp)	# paired reads	Total length (Gb)	Coverage (~ 20 Mb)	# Contigs	# Scaffolds (≥ 500 bp)	Scaffold N50	Largest Scaffold (bp)	Genome assembly size (bp)	GC%
CBS 5930	2 x 100	282	25,043,726	2.5	125 x	2 x 100	3506	10,699,370	1.1	53 x	3,730	828	244,613	712,619	26,913,765	59.0
CBS 5931	2 x 100	270	27,880,624	2.8	139 x	2 x 100	3709	15,436,512	1.5	77 x	3,788	921	169,176	869,953	26,913,583	59.0

Table S3 List of primers and specific PCR conditions used in this study.

Region/gene	Primers	Sequence (5' > 3')	Annealing / Extension (° / sec)	Remarks
STE3.A1	TM1-LsSTE3.A1_1294_F TM2-LsSTE3.A1_2231_R	TTCAACTTCCTGGCCATCCTGTTC TCGCCGAGCCCGAAGAAGAGG AAG	62.0 / 60	Detection of *MAT* A1 allele
STE3.A2	TM3-LsSTE3.A2_53_F TM4-LsSTE3.A2_1074_R	TCGCCGAGCCCGAAGAAGAGGAAG AATGCCGGCCCGCTTTACTGGCA	65.0 / 90	Detection of *MAT* A2 allele
HD1/HD2	TM24_HD1R TM26_HD2R	CGGCMGGTRTTGATRAACCA CCANGTNCCGACCTGCTTCTC	60.0 / 120	Amplification and sequencing 5' end and intergenic regions of the *HD1* and *HD2* genes
RHA.A1	MAD4-PRE3F MAD5-RHAF	CAGATTACCGTGACGGAGGT GTCCCCCGTTCAGCTCTC	57.0 / 60	Amplification and sequencing of the pheromone precursor gene *RHA.A1*
3' end of *HD1*	TM30_HD1pF TM31_HD1pR	ACAAGAAAGCCCTCCACCTC CTTGAGATCCTCCTCGAACG	57.0 / 60	Probe for chromosomal detection of the *HD* locus
STE20	TM28-STE20pF TM29-STE20pR	TTATCCAGCTACGGGACCTC CTGTCCTGCGAATCCAGTG	58.0 / 90	Probe for chromosomal detection of the *P/R* locus

PCR reactions were performed in a final volume of 10 μl with the following components: 1X DreamTaq Buffer (Fermentas, Canada), 0.20 mM of each of the four dNTPs (GE Healthcare), 1% DMSO, 0.4 μM of each primer, 200 ng of genomic DNA, and 0.5 U DreamTaq DNA polymerase (Fermentas, Canada). Thermal cycling consisted of a 5-minute denaturation step at 95°, followed by 35 cycles of denaturation at 95° for 30 s, 30 s at the annealing temperature (variable), and extension at 72° (variable time). The annealing temperatures, extension times and primer sequences are given for each case. A final extension of 7 min at 72° was performed at the end of each reaction. PCRs reactions were adjusted to 50 μl final volume when sequencing was required.

Table S4 Mating assays for *L. scottii* strains with previously undescribed fertility.

MAT A1 Strains		*MAT A2* Strains: CBS 5930	UFMG-ANT 158	UFMG-ANT 160	CBS 7673	CBS 9490	PYCC 4751	PYCC 4754	PYCC 4755	CBS 4025	CBS 4026	CBS 2300	(a)
		A2B2	A2B2	A2B2	A2B19	A1A2 B19	A2B22	A2B22	A2B14	A2B24	A2B24	A1A2 B23	
CBS5931	A1B1	+++	+++	+++	+++	++	+	–	+	–	–	+++	–
UFMG-EACF149	A1B10	+++	++	+++	–	+	–	–	–	–	+	–	–
UFMG-ANT 139	A1B10	+++	+++	+	–	–	–	–	–	–	–	–	–
CBS 5932	A1B3	+	++	++	++	–	–	–	+	+	–	–	– (b)
CBS 8039	A1B3	++	+++	–	++	++	+	–	+	–	–	–	–
CBS 614	A1B5	+++	++	+++	+++	+++	++	–	–	+++	+++	+++	– (b)
CBS 8036	A1B17	+++	+++	+++	+++	+++	++	+++	–	–	–	+++	–
CBS 9965	A1B18	++	+++	++	++	–	–	–	–	–	–	–	– (c)
PYCC 4696	A1B13	+++	+++	+++	+++	–	–	–	–	–	–	+++	–
PYCC 4509	A1B13	+++	+++	+++	+++	+++	–	–	++	–	–	–	–
PYCC 4508	A1B15	+	–	+	++	+	–	–	–	–	–	–	–
PYCC 4510	A1B16	++	+++	+++	++	++	+	–	–	–	+	++	–
CBS 8188	A1B29	–	+++	–	–	+	+	–	–	–	–	–	–
CBS 8633	A1B26	+	+	+++	–	–	–	–	+	–	++	++	–
CBS 10581	A1B25	–	–	–	–	–	–	–	–	–	–	–	–
CBS 9467	A1B23	+	+	+	–	–	–	–	–	–	–	–	–
CBS 2300	A1A2B23	–	–	–	–	–	–	–	–	–	–	–	–
(a)		–	–	–	–	–	–	–	–	–	–	–	–

Results are from two independent tests. Production of mycelium and teliospores was classified as extensive when these structure covered all the area of the mating plate (+++), moderate when restricted to a few areas of the plate (++), poor when these structures were only detected in a single spot and took longer time to form (+), and negative (–).

(a) No mating partner was added in order to test for self-fertility.

(b) Strain reported to be self-fertile by Fell and Statzell-Tallman 1982.

(c) Strain reported to be self-fertile by de Garcia et al. 2015.

Table S5 Molecular mating type of the meiotic progeny recovered from cross CBS 5931 x CBS 5930.

#F1 progeny	*MAT* genotype	#Teliospore
#Ls001	A1A2B1B2	1
#Ls006	A2B2	2
#Ls016	A1A2B1B2	3
#Ls017	A1B1	
#Ls022	A2B1B2	
#Ls013	A2B1	4
#Ls025	A1A2B2	
#Ls031	A2B2	
#Ls037	A1A2B1B2	5
#Ls039	A1A2B1	
#Ls040	A1A2B1B2	6
#Ls044[(a)]	A1A2B1B2	7
#Ls048	A1A2B1B2	8
#Ls052	A2B1B2	9
#Ls053	A2B2	10
#Ls056	A2B2	11
#Ls058	A2B1	12
#Ls062	A2B1	13
#Ls066[(a)]	A1A2B1B2	14
#Ls070	A2B2	15
#Ls072[(a)]	A1A2B1	16
#Ls073	A1A2B1B2	
#Ls074	A2B2	
#Ls077	A1A2B1B2	17
#Ls078	A1B1	
#Ls081	A2B1B2	18
#Ls084	A1A2B1B2	
#Ls086	A2B1B2	19
#Ls088	A2B1	
#Ls089	A1A2B1	
#Ls090	A2B1	20
#Ls092	A2B1B2	
#Ls093	A2B1	21
#Ls094	A1A2B1B2	22
#Ls095	A1A2B1B2	23
#Ls096	A2B1B2	
#Ls097	A1B1B2	24
#Ls101	A1B1	
#Ls103	A2B2	25
#Ls105[(a)]	A2B1B2	
#Ls108	A1A2B1B2	26
#Ls112	A1B1B2	27
#Ls114	A1A2B1B2	28
#Ls115	A2B1B2	
#Ls118	A1B2	29
#Ls120	A1A2B2	30
#Ls121	A2B1B2	31
#Ls127	A1B1B2	32
#Ls128	A1A2B1B2	33
#Ls130	A1A2B1B2	34
#Ls132	A1A2B1B2	35
#Ls133	A1B1	
#Ls136	A1A2B1B2	36
#Ls142	A1B1B2	
#Ls143	A1A2B1	37
#Ls149	A1A2B1B2	38
#Ls152	A1A2B1B2	39
#Ls153	A1A2B1B2	40
#Ls159	A1A2B1B2	41
#Ls168[(a)]	A1B1B2	42
#Ls173	A1A2B1	43
#Ls175	A1A2B1B2	
#Ls177	A1A2B1B2	44
#Ls181	A1A2B1B2	45
#Ls192	A1A2B1B2	46
#Ls206	A1A2B1B2	47
#Ls207	A1B1	48
#Ls219	A1B1B2	49
#Ls223	A1B2	50
#Ls224	A1A2B2	
#Ls226	A2B2	
#Ls227	A1B1	

(a) F1 progeny used to assess ploidy and fertility changes after mitotic passages.

Table S6 Fertility of meiotic progeny from cross CBS 5931 x CBS 5930.

		Tester strains				
		CBS 5931	CBS 5930	CBS 6561	CBS 6562	(a)
F1 progeny	*MAT*	A1B1	A2B2	A1B2	A2B1	
#LS017	A1B1		+++			–
#LS078			++			–
#LS101			–			–
#LS207			++			–
#LS227		–	++	–	–	–
#LS031	A2B2	++				–
#LS053		–				–
#LS056		+				–
#LS074		+				–
#LS226		++	–	–	–	–
#LS118	A1B2				++	–
#LS223		–	–	–	–	–
#LS013	A2B1			+++		–
#LS058				+		–
#LS062				++		–
#LS088				+++		–
#LS090				++		–
#LS039	A1A2B1		+++	++		–
#LS072			++	+		–
#LS089			+	+		–
#LS143			+	++		–
#LS025	A1A2B2	++			+	–
#LS120		++			–	–
#LS224		+	–	–	–	–
#LS142	A1B1B2		++		+	++
#LS168			++		+	++
#LS219			–		+	++
#LS081	A2B1B2	+		++		–
#LS086		–		+		–
#LS092		+		+		–
#LS105		+		++		+
#LS108	A1A2B1B2					+++
#LS136						+++
#LS159						+++
#LS181						+++
#LS192						+++
#LS044						+++
#LS066						+++

Results are from two independent tests. Production of mycelium and teliospores was classified as extensive when these structure covered all the area of the mating plate (+++), moderate when restricted to a few areas of the plate (++), poor when these structures were only detected in a single spot and took longer time to form (+), and negative (–). Crosses not assessed are marked in grey.

(a) No mating partner was added in order to test for self–fertility.